Annual Review of Biochemistry

Mechanisms of Vertebrate DNA Interstrand Cross-Link Repair

Daniel R. Semlow[1,2] and Johannes C. Walter[1,3]

[1]Department of Biological Chemistry and Molecular Pharmacology, Blavatnik Institute, Harvard Medical School, Boston, Massachusetts 02115, USA; email: johannes_walter@hms.harvard.edu

[2]Current affiliation: Division of Chemistry and Chemical Engineering, California Institute of Technology, Pasadena, California 91125, USA

[3]Howard Hughes Medical Institute, Harvard Medical School, Boston, Massachusetts 02115, USA

Annu. Rev. Biochem. 2021. 90:107–35

First published as a Review in Advance on April 21, 2021

The *Annual Review of Biochemistry* is online at biochem.annualreviews.org

https://doi.org/10.1146/annurev-biochem-080320-112510

Keywords

Fanconi anemia, DNA interstrand cross-link, FANCD2, ICL, NEIL3, traverse

Abstract

DNA interstrand cross-links (ICLs) covalently connect the two strands of the double helix and are extremely cytotoxic. Defective ICL repair causes the bone marrow failure and cancer predisposition syndrome, Fanconi anemia, and upregulation of repair causes chemotherapy resistance in cancer. The central event in ICL repair involves resolving the cross-link (unhooking). In this review, we discuss the chemical diversity of ICLs generated by exogenous and endogenous agents. We then describe how proliferating and nonproliferating vertebrate cells unhook ICLs. We emphasize fundamentally new unhooking strategies, dramatic progress in the structural analysis of the Fanconi anemia pathway, and insights into how cells govern the choice between different ICL repair pathways. Throughout, we highlight the many gaps that remain in our knowledge of these fascinating DNA repair pathways.

Contents

INTRODUCTION

In the early twentieth century, it was discovered that mustard gas, a bifunctional alkylating agent, is highly damaging to hematopoietic cells, which was the first indication that such agents could be used in cancer therapy (1). The subsequent observation that bifunctional alkylators are much more cytotoxic than monofunctional agents suggested that cytotoxicity derives from the cross-linking of macromolecules involved in cell division. The model of DNA and its mode of duplication proposed in 1953 immediately suggested that cross-linking between the two DNA strands might underlie the cytotoxicity of alkylating agents. The first evidence for this idea came soon thereafter with the finding that nitrogen mustards cross-link guanines (2). Since then, diverse bifunctional cross-linking agents have been identified, many of which are now used in cancer therapy (3). Importantly, endogenous metabolites also create interstrand cross-links (ICLs), which explains why cells have evolved elaborate mechanisms to repair these dangerous lesions. Hereditary mutations in genes required for ICL repair cause cancer and bone marrow failure, and there is evidence that somatic mutations in these genes also contribute to cancer progression (4). On the other hand, upregulation of ICL repair in tumors is associated with chemotherapy resistance (4). Thus, understanding the molecular basis of ICL repair is highly relevant to cancer biology. The critical event in all forms of ICL repair is called unhooking, in which the covalent linkage between the two strands of DNA is resolved. In this review, we present an updated description of how ICLs are formed by exogenous and endogenous agents. We then discuss how vertebrate cells repair ICLs. We emphasize the three known pathways of replication-coupled ICL repair, since these are the most critical for cell survival, and we contrast these with replication-independent pathways of ICL repair.

SOURCES OF ICLs

ICLs are generated by diverse chemical agents and mechanisms (**Figure 1**). The structural diversity of ICLs arises as a function of the myriad agents that can form DNA adducts, coupled with

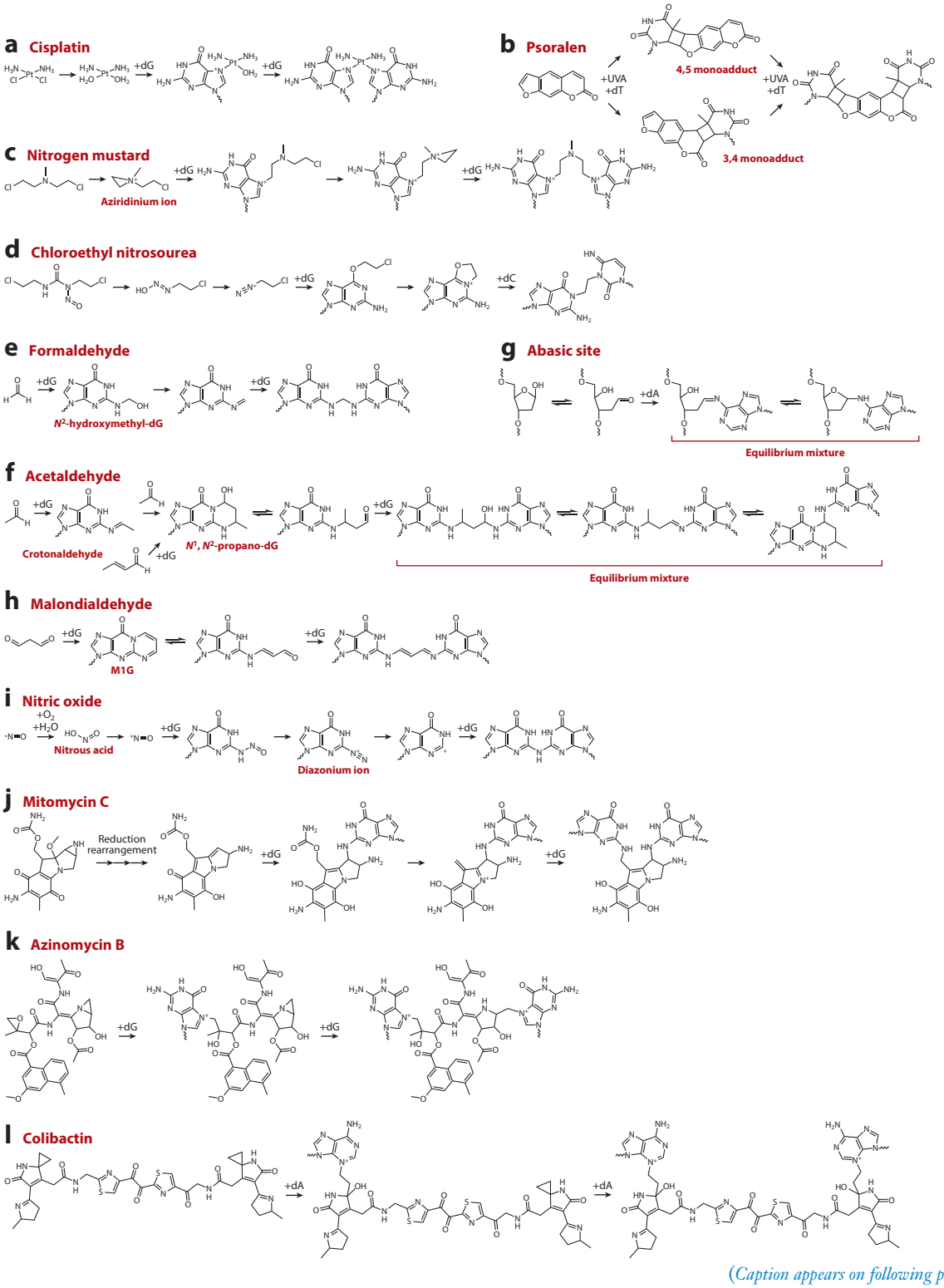

(*Caption appears on following page*)

Figure 1 (*Figure appears on preceding page*)

Mechanisms of interstrand cross-link (ICL) formation. (*a*) Platinum compounds (e.g., cisplatin, carboplatin, oxaliplatin) contain a *cis* arrangement of two chlorido ligands that are displaced by water in cells. This activated form reacts predominantly with the N^7 position of dG to adduct DNA (153). Subsequent reaction at N^7 of a second dG on the same strand produces a DNA intrastrand cross-link, whereas reaction with the opposing strand produces an ICL. (*b*) Psoralen and its derivatives (e.g., trimethylpsoralen and 8-methoxypsoralen) are composed of aromatic fused furan and pyrone structures. Psoralens intercalate into DNA, and photoactivation with ultraviolet light generates cyclobutane adducts with the 5,6 double bond of deoxythymidine on either the furan side (4,5 monoadduct) or pyrone side (3,4 monoadduct) (154). Reaction of the same psoralen with two deoxythymidines on opposing strands produces a psoralen ICL that does not significantly distort the DNA helix (155). (*c*) Nitrogen mustards (e.g., chlorambucil, cyclophosphamide, melphalan) undergo intramolecular activation to generate aziridinium ions that can alkylate the N^7 and O^6 positions of dG, the N^3 and N^1 positions of dA, and the N^3 position of dC (summarized in 156). Reaction of nitrogen mustards with DNA has been observed to produce dG–dG, dG–dA, and dA–dA cross-links (157, 158). (*d*) Chloroethyl nitrosoureas (e.g., carmustine and lomustine) initially react at the O^6 position of dG and then undergo cyclization with the N^1 position. This adduct can then be attacked by the N^3 position of dC to form a dG–dC ICL (159). (*e*) Formaldehyde (from one carbon metabolism and DNA and histone demethylation) reacts with the N^2 exocyclic amine of dG to produce a hydroxymethylguanine adduct and subsequent Schiff base intermediate that can be attacked by a second exocyclic amine at the N^2 position of dG to cross-link the two nucleotides through a methylene bridge (9). (*f*) Reaction of two acetaldehyde molecules (from alcohol metabolism) or a single crotonaldehyde molecule (from lipid peroxidation) with dG forms a cyclic N^1,N^2-propanoguanine monoadduct (160). Further reaction with a second dG produces dG–dG ICLs that exist as equilibrium mixtures of cyclized and extended forms (161). (*g*) The aldehyde form of an abasic site (from spontaneous depurination events or DNA glycosylase action) reacts with the exocyclic amine of dA to produce an ICL that exists as an equilibrium mixture of deoxyribose ring-open and ring-closed forms (162). (*h*) Malondialdehyde (from lipid peroxidation) reacts with N^2 of dG, generating an M1G adduct that can isomerize and further react to form a dG–dG ICL (163). (*i*) Nitric oxide is converted to nitrous acid, which reacts with DNA exocyclic amines in vitro to generate ICLs via a diazotized intermediate (164). (*j*) The *Streptomyces caespitosus* isolate mitomycin C (MMC) is unreactive toward DNA until it is activated through chemical or enzymatic reduction (165). Reduction of MMC induces a series of rearrangements that result in formation of a vinyl group that reacts with the N^2 of dG to generate the dominant MMC monoadduct. A subsequent rearrangement of the monoadduct produces a second vinyl that reacts with N^2 of a second dG to form an ICL. (*k*) Produced through a polyketide synthase–nonribosomal peptide synthetase (PKS-NRPS) biosynthetic pathway, azinomycin B contains epoxide and aziridine rings that each react with the N^7 positions of purines to cross-link DNA (166, 167). (*l*) Colibactin, produced by bacteria expressing a PKS-NRPS gene cluster (168), binds in the minor groove of DNA and contains two cyclopropane groups that react with the N^3 position of dA in opposing strands to form ICLs (13, 14).

the multiple reactive functional groups found on DNA nucleobases. Although preferred adduction sites vary with the genotoxic agent, purine nucleotides (dG and dA) tend to be more reactive than pyrimidine nucleotides (dT and dC) (5), and purines, especially dG, make up the majority of physiologically and therapeutically relevant ICLs. However, all four DNA nucleotides have been observed to participate in cross-link formation. In general, cross-links form between adjacent DNA functional groups that occupy the same major or minor DNA groove, though longer cross-linking agents (e.g., nitrogen mustards) can span intervening nucleotides. In addition, some ICLs cause dramatic DNA unwinding, helical bends, and even eversion of adjacent bases, while others produce minimal perturbations (6). Importantly, the degree of ICL-induced DNA distortion influences the choice of ICL repair pathway (7).

ICL-inducing agents can be loosely classified as chemotherapeutics, endogenous metabolites, or microbial metabolites. Cross-linking drugs used in chemotherapy include platinum compounds, psoralens, nitrogen mustards, and chloroethyl nitrosoureas (**Figure 1*a–d***). Cisplatin, for example, preferentially reacts at the N^7 position of dG to generate both intrastrand and highly distorting interstrand cross-links (8). Endogenous sources of ICLs include, predominantly, electrophilic aldehydes that typically react with the exocyclic amines of purine nucleotides (the N^2 position of dG and N^6 position of dA). In the case of formaldehyde (**Figure 1*e***), nucleophilic attack by an exocyclic amine forms a hydroxymethyl monoadduct that can further react to produce an ICL with a second exocyclic amine (9). Importantly, a di(N^2-guanosyl)methane cross-link formed by endogenous formaldehyde is currently the only endogenous ICL reported to have been detected in tissues (10). Acetaldehyde, malondialdehyde, and abasic [or apurinic/apyrimidinic (AP)]

site aldehydes form ICLs by analogous chemical mechanisms (**Figure 1*f–b***). Other endogenous species, such as the signaling molecule nitric oxide (**Figure 1*i***), can also form ICLs, though the physiological significance of ICLs produced by these agents remains largely unexplored. ICL-inducing agents produced by bacteria have found clinical relevance both as chemotherapeutics and as potential drivers of human disease (**Figure 1*j–l***). The widely used chemotherapeutic mitomycin C (**Figure 1*j***), which cross-links the N^2 position of dG, was originally isolated from *Streptomyces caespitosus* and is still produced from bacterial extracts (11). Azinomycin B is another *Streptomyces* isolate with antitumor properties that derive from its ability to form ICLs (12). More recent work has revealed that colibactin (**Figure 1*l***), an *Escherichia coli* toxin associated with colorectal cancer, is a bifunctional alkylating agent that forms cross-links through reaction at the N^3 position of dA (13, 14). Importantly, DNA adduction by colibactin can induce rapid depurination, resulting in AP sites that can decompose into single-strand and double-strand DNA breaks (DSBs) (15). Colibactin is therefore likely to produce a complicated spectrum of DNA damage requiring multiple mechanisms of DNA repair. This variety of ICL structures probably helps to account for the multiple pathways, described below, that vertebrate cells possess to repair these lesions.

REPLICATION-DEPENDENT ICL REPAIR

ICLs impede DNA replication, with potentially catastrophic consequences. It is therefore not surprising that DNA replication forks trigger ICL repair. Cells prepare for replication in the G1 phase of the cell cycle when many prereplication complexes consisting of minichromosome maintenance 2–7 (MCM2–7) double hexamers are assembled along vertebrate chromosomes (16). In S phase, MCM2–7 double hexamers are activated by cyclin-dependent kinase, leading to the association of cell division cycle 45 (CDC45) and go-ichi-ni-san (GINS) with MCM2–7 and formation of the Cdc45-MCM2–7-GINS (CMG) helicase. CMG translocates along the leading strand template, unwinding DNA at the leading edge of the replisome. As described below, all known mechanisms of replication-coupled ICL repair are initiated by collision of CMG with the lesion.

THE FANCONI ANEMIA PATHWAY

The first mechanism of replication-coupled ICL repair discovered in mammalian cells has come to be known as the Fanconi anemia (FA) pathway (17). In 1927, the Swiss pediatrician Guido Fanconi described three siblings that exhibited birth defects and severe anemia (18). Later, it was appreciated that FA is also associated with acute myeloid leukemia as well as solid tumors of the head and neck. In 1973, Sasaki and Tonomura discovered that, upon exposure to bifunctional cross-linking agents, FA patient–derived cells exhibit a high level of chromosomal aberrations, indicative of a defect in repair (reviewed in 19). Together, these results established FA as a genome instability syndrome characterized by congenital abnormalities, bone marrow failure, and cancer predisposition. FA is an autosomal recessive disorder, and to date, mutations in 22 different *FANC* genes have been associated with the disease (4) (**Figure 2**). Several lines of indirect evidence suggest that FA is caused by a defect in the repair of ICLs generated by endogenous aldehydes (20) (**Supplemental Appendix 1**). However, it has not been demonstrated that endogenous ICLs accumulate in FA cells, so this model requires confirmation.

Supplemental Material >

We classify the 22 Fanconi gene products into four functional groups (**Figure 2**). Many of the FANC proteins had been previously identified, and in the following description, their original names are given in parentheses. We also highlight proteins that interact closely with the FANC proteins but do not carry the FANC designation because mutations in the corresponding genes have not yet been linked to FA. The first group is called the FANCM module and

#	Group	FANC protein	Alias	Function
1	1	M	-	DNA translocase
2	2	A	-	E3 Ubiquitin ligase for ID
3	2	B	-	E3 Ubiquitin ligase for ID
4	2	C	-	E3 Ubiquitin ligase for ID
5	2	E	-	E3 Ubiquitin ligase for ID
6	2	F	-	E3 Ubiquitin ligase for ID
7	2	G	-	E3 Ubiquitin ligase for ID
8	2	L	-	E3 Ubiquitin ligase for ID
9	2	T	UBE2T	E2 for ID
10	3	D2	-	ID complex
11	3	I	-	ID complex
12	4	P	SLX4	XPF-binding protein
13	4	Q	XPF	Endonuclease (NER)
14	4	D1	BRCA2	Recombination
15	4	O	RAD51C	Recombination
16	4	R	RAD51	Recombination
17	4	U	XRCC2	Recombination
18	4	N	PALB2	Recombination
19	4	S	BRCA1	Recombination
20	4	J	BRIP1	DNA Helicase
21	4	W	RFWD3	E3 ubiquitin ligase
22	4	V	REV7	TLS polymerase

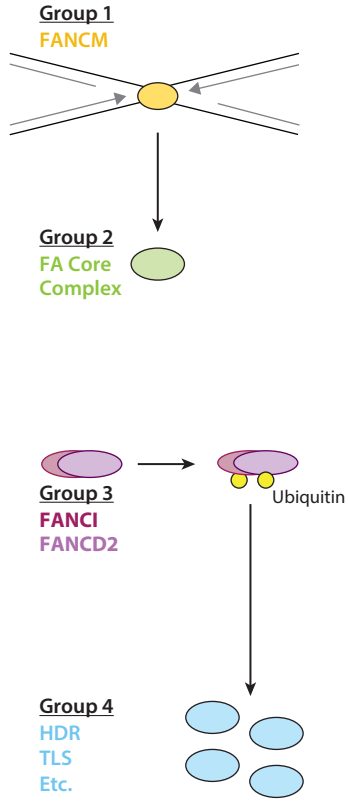

Figure 2

The FANC proteins. The 22 FANC proteins can be divided into four groups based on their proposed functions in ICL repair. Where applicable, the alternative name is indicated (Alias). Abbreviations: FA, Fanconi anemia; ICL, interstrand cross-link; TLS, translesion synthesis.

includes the ATPase FANCM as well as its three main interacting partners, Fanconi-associated protein 24 (FAAP24) and the histone fold proteins MHF1 and MHF2 (21). This heterotetrameric FANCM complex recognizes stressed replication forks and helps recruit the group 2 proteins, which form a large E3 ubiquitin ligase called the FA core complex. The core complex is composed of FANCA, B, C, E, F, G, L, FAAP20, and FAAP100. The core recruits FANCT (UBE2T), a ubiquitin-conjugating enzyme that monoubiquitylates a heterodimer of the two group 3 proteins, FANCI and FANCD2 (the ID complex). While FANCD2 ubiquitylation on K561 is essential for ICL repair, FANCI ubiquitylation on K523 plays a regulator role, as described below (22, 23). Monoubiquitylated ID (ID^{Ub}) forms nuclear foci that colocalize with components of the recombination machinery and presumably represent sites of repair (24). Group 4 includes the proteins that perform DNA repair and DNA damage bypass. These include FANCP (SLX4), a large scaffolding protein that interacts with the structure-specific endonuclease FANCQ (XPF)-ERCC1 that unhooks the ICL; FANCD1 (BRCA2), FANCO (RAD51C), FANCR (RAD51), FANCU

(XRCC2), FANCN (PALB2), and FANCS (BRCA1), all of which play well-established roles in homology-directed repair; the E3 ubiquitin ligase FANCW (RFWD3) and the 3′ to 5′ DNA helicase FANCJ (BRIP1/BACH1), both of which have been implicated in homologous recombination (25, 26); and FANCV (REV7), which, together with REV3, forms the translesion synthesis (TLS) DNA polymerase ζ (Pol ζ). In summary, the 22 FANC proteins include a damage-sensing module (group 1), an E3 ubiquitin ligase (group 2) that ubiquitylates the effector ID complex (group 3), and a large group of DNA repair/damage tolerance factors (group 4), which are not required for ID ubiquitylation.

An Early Model of the Fanconi Anemia Pathway

The first model of ICL repair by the FA pathway emerged from four early insights. First, ICL repair is coupled to DNA replication (reviewed in 27). In support of this notion, ICL-inducing agents cause cells to arrest in late S phase with G2 DNA content. Moreover, these agents promote the formation of DSBs, but only upon S phase entry. Finally, ubiquitylation of FANCI-FANCD2 is strictly coupled to DNA replication. The second key insight was that ICL repair involves homologous recombination. This was based on the findings that the *FANCD1* gene encodes the recombinase BRCA2 and that, in chicken cells, FANCC and the RAD51 paralog XRCC2 are epistatic (28, 29). Third, FA cells undergo reduced spontaneous and ICL-induced mutagenesis (30, 31), and the TLS DNA polymerase Rev1 exhibits genetic epistasis with FANCC for ICL repair (29), suggesting the FA pathway includes a TLS event. Fourth, cells deficient in the structure-specific endonuclease XPF, originally identified as a nucleotide excision repair protein, are highly sensitive to ICLs (32). Together, these observations supported a model in which the collision of replication forks with an ICL triggers XPF-ERCC1-dependent DNA incisions that unhook the ICL and generate a DSB (33) (**Figure 3*a***, **subpanel *i***). Repair is completed when a TLS polymerase bypasses the monoadduct generated by unhooking (**Figure 3*a***, **subpanel *ii***), the monoadduct is removed by excision repair (**Figure 3*a***, **subpanel *iii***), and homologous recombination restores the replication fork (**Figure 3*a***, **subpanels *iv–v***). This model accounted for key genetic and cytological observations and motivated work in the field for many years.

Activation of ICL Repair by Replication Fork Convergence

In 2008, repair of a plasmid containing a site-specific cisplatin ICL site was recapitulated in *Xenopus* egg extracts (34), laying the foundation for a mechanistic analysis of ICL repair. In this system, the initiation of repair requires the convergence of two replication forks on the ICL (35) (**Figure 3*b***, **subpanel *i***). Fork convergence triggers ubiquitylation of the CMG helicase by the E3 ubiquitin ligase TRAIP (36), whose loss sensitizes mammalian cells to cross-linking agents (37–39). Once ubiquitylated, CMG is unloaded from the chromatin by the p97 ATPase (36, 40) (**Figure 3*b***, **subpanel *ii***). CMG unloading allows one fork to undergo reversal (41) (**Figure 3*b***, **subpanel *iii***), but it might also be critical to expose the fork for nucleolytic cleavage. Although purified FANCM promotes reversal of model DNA templates (42), a role for FANCM in fork reversal at ICLs has not been documented. Without the identification of a specific fork reversal enzyme, it has been impossible to ascertain whether reversed forks represent an essential intermediate in ICL repair.

Collision of forks with the ICL leads to the generation of ID^{Ub} (34), which binds near the ICL and promotes ICL unhooking by recruiting the scaffolding protein FANCQ (SLX4) (43–45) (**Figure 3*b***, **subpanel *iv***). Whether ID^{Ub} also recruits SLX4 to sites of damage in cells is controversial (46, 47). SLX4's MUS312/MEI9 interaction-like region (MLR) domain binds and recruits XPF-ERCC1, a 3′ flap endonuclease that is critical for unhooking (43, 48), as seen also in cells (32, 49–52). Importantly, purified XPF does not cleave X-shaped structures, whereas it readily cleaves

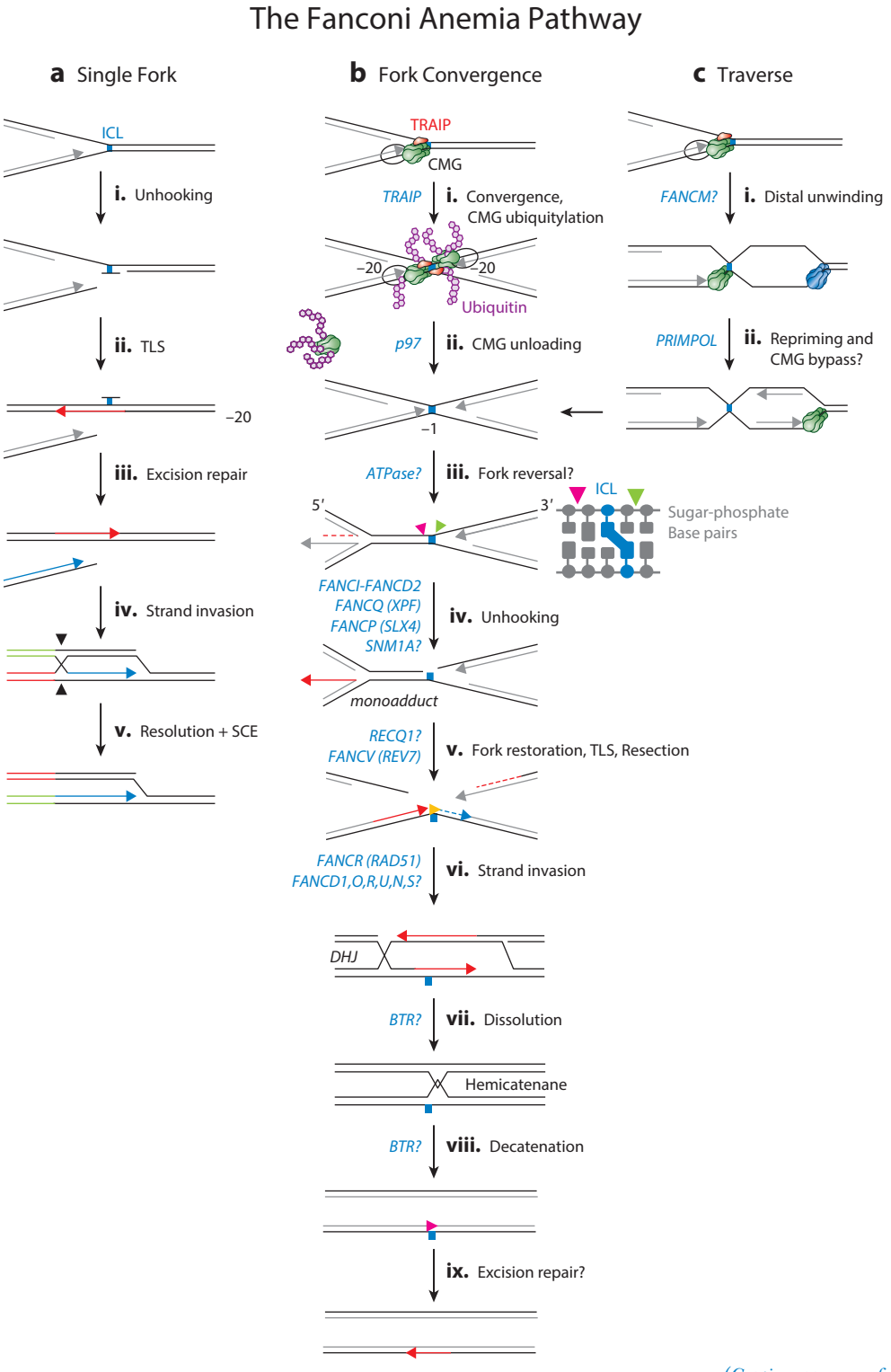

(Caption appears on following page)

Figure 3 (*Figure appears on preceding page*)

Three models of ICL repair via the Fanconi anemia pathway. (*a*) The early model, in which a single replication fork triggers ICL repair (33). (*b*) Fork convergence model. The importance of fork reversal for ICL repair (*iii*) has not been clearly established because the ATPase responsible has not been identified. Pink and green arrowheads indicate XPF and SNM1A incisions, respectively. The yellow arrowhead indicates an insertion of a nucleotide across from the unhooked monoadduct. (*c*) Model of replication traverse. Abbreviations: BTR, BLOOM-TOP3A-RMI1-RMI2 complex; CMG, CDC45-MCM2–7-GINS; DHJ, double Holliday junction; ICL, interstrand cross-link; SCE, sister chromatid exchange; TLS, translesion synthesis.

fork structures several nucleotides from the single-stranded DNA (ssDNA)–double-stranded DNA (dsDNA) junction (41, 53) (see the pink arrowhead in **Figure 3*b***, **subpanels *iii***). This observation suggests that fork reversal might convert X-shaped DNA into an appropriate structure for XPF cleavage. At present, the nuclease that incises the other side of the ICL is unknown (54) (see the green arrowhead in **Figure 3*b***, **subpanel *iii***). While XPF has been proposed to incise both sides of an ICL (55–57), such a mechanism is difficult to reconcile with its propensity to cleave forks within duplex DNA. Moreover, current evidence disfavors essential roles for FAN1, SLX1, or MUS81 in ICL repair by the FA pathway (**Supplemental Appendix 2**). In contrast, SNM1A is an excellent candidate. This nuclease has the appropriate specificity, being able to degrade a DNA strand past an ICL starting from an incision on the 5′ side of the lesion, such as would be made by XPF (58). Additionally, genetic epistasis suggests that in mammalian cells, SNM1A collaborates with XPF in ICL repair (58), and SNM1A correlates highly with FANC genes in genome-wide CRISPR (clustered regularly interspaced short palindromic repeat) screens (39). The fact that SNM1A depletion itself causes moderate ICL sensitivity (59) could be due to redundancy with another nuclease such as FAN1 (60, 61).

Supplemental Material >

Cell-free ICL repair allowed leading-strand bypass of the lesion to be monitored at nucleotide resolution (34). Upon initial fork stalling, leading strands arrest 20–40 nucleotides from the ICL due to the CMG footprint (35) (**Figure 3*b***, **subpanel *i***). Once CMG is unloaded, leading strands advance to within one nucleotide of the ICL (**Figure 3*b***, **subpanel *ii***), but whether one or both leading strands advance is unclear. The polymerase that inserts a nucleotide across from the unhooked ICL (**Figure 3*b***, **subpanel *v***) has not been identified. Generally, the insertion polymerase probably depends on the chemical structure of the ICL, and for some ICLs, there appears to be redundancy between TLS polymerases and possibly replicative polymerases (62). After the insertion step, a complex of the scaffold REV1 (a deoxycytidine monophosphate transferase) and Pol ζ extends the leading strand past the ICL remnant (34, 63) (**Figure 3*b***, **subpanel *v***). This is consistent with genetic studies demonstrating the exquisite sensitivity of REV1, REV3, and REV7 mutant mammalian cells to ICL-inducing agents, as well as biochemical studies showing that Pol ζ often promotes strand extension beyond an abnormal base pair (62). Interestingly, evidence in extracts and cells indicates that TLS is stimulated by the FA core complex independently of ID ubiquitylation (63, 64). After extension, the leading strand is ligated to the downstream Okazaki fragment of the converging fork (**Figure 3*b***, **subpanel *v***, dotted arrow). If incisions require prior fork reversal, then once incisions have occurred, the leading strand would need to be restored to its original location before TLS can take place (**Figure 3*b***, **subpanel *v***). It is unknown which proteins would support restoration, but RECQ1 is an attractive candidate (65).

The next event in cell-free ICL repair is homologous recombination. The two-ended DSB generated by unhooking (and possibly restoration of a reversed fork; **Figure 3*b***, **subpanel *v***) is repaired by Rad51-dependent homologous recombination (66) (**Figure 3*b***, **subpanel *vi***). In cells, this process likely requires FANCD1 (BRCA2), FANCO (RAD51C), FANCR (RAD51), FANCU (XRCC2), FANCN (PALB2), and FANCS (BRCA1) (4, 17, 67) (**Figure 2**). Before strand invasion can occur, the ends of the DSB must be resected to produce 3′ ssDNA overhangs for assembly of

the RAD51 presynaptic filament. Resection of nascent lagging strands begins soon after forks converge and depends on CMG unloading (34, 41) (see the dashed red line in **Figure 3*b*, subpanel *iii***). The enzymes that perform resection in this system are unknown, but in mammalian cells, the process depends on Dna2, Exo1 (68), and possibly the Werner DNA helicase (69), whose activities are carefully regulated to prevent over-resection (70–72). Strand invasion into the intact sister chromatid likely produces a double Holliday junction (DHJ) (**Figure 3*b*, subpanel *vi***), whose subsequent dissolution forms a mobile hemicatenane (66) (**Figure 3*b*, subpanel *vii***). Dissolution and decatenation probably depend on the BLM-TOPO3α-RMI1-RMI2 (BTR) complex (73–75). Interestingly, in egg extracts, RAD51, BRCA1, and BRCA2 bind to chromatin prior to ID-dependent incisions, consistent with cell-based studies demonstrating that RAD51 focus formation does not require incisions (19). The function of preincision recombinase binding is unclear, but it might initiate recombination before strand breakage (3) or help suppress aberrant nascent strand degradation by DNA2 and the WRN helicase (71, 72).

Once the DSB has been fixed, the remnant of the ICL remains attached to one strand of the two sister chromatids. In egg extracts, this monoadduct remains on the DNA indefinitely (34). In cells, both base excision repair and nucleotide excision repair have been implicated in the removal of monoadducts, and which pathway is used likely depends on the structure of the adduct (27) (**Figure 3*b*, subpanel *ix***).

Traverse

The use of a small plasmid to study ICL repair in egg extracts leads inevitably to rapid fork convergence. The question arises of how forks interact with ICLs in cells, where the average interorigin distance is approximately 100 kb (76). To address this, Seidman and colleagues (77) performed DNA combing to simultaneously visualize ICLs and the directionality of replication forks. As expected, some ICLs (~20%) abutted a single replication fork, whereas others were sandwiched between converging forks (~15%). Surprisingly, in about 60% of cases, a single replication fork passed through the intact ICL (traverse), suggesting that, unlike in egg extracts, the replication machinery can bypass an ICL in cells (**Figure 3*c***).

Traverse takes only about 5 min and depends on FANCM-MHF1-MHF2 (but not FAAP24), FANCM's ATPase activity, the BTR complex, FANCI-FANCD2 (but not its ubiquitylation), the checkpoint kinase ATR, and PRIMPOL (77–79). Traverse is associated with displacement of the GINS subunit from the CMG helicase at the ICL, which depends on ATR phosphorylation of FANCM and its interaction with the MCM2–7 complex, but not on FANCM ATPase activity (79). A possible model is that GINS displacement allows the CMG ring to open so it can bypass the ICL and continue unwinding beyond the lesion, followed by PRIMPOL-dependent repriming of the leading strand beyond the ICL. However, direct evidence that CMG unwinds DNA beyond the ICL is lacking. Importantly, CMG bypass of DNA protein cross-links occurs in the absence of GINS dissociation (80). We suspect that CMG uses the same mechanism to bypass ICLs, DPCs, and any other bulky lesions on the translocation strand. For example, bypass may involve opening of a CMG gate that resides distal to the GINS and CDC45 binding sites on the MCM2–7 ring, as recently proposed (81). The role of FANCM's ATPase activity in traverse is unclear. One possibility is that FANCM and/or BLM cooperate to unwind DNA beyond the ICL to allow reengagement of CMG or recruitment of a new helicase (75, 78, 82) (**Figure 3*c***). Because FANCM ATPase activity is not required for FANCD2 ubiquitylation (83), its essential function in ICL repair might be in promoting traverse. Although it has been proposed that traverse requires prior fork reversal (84), the mechanistic basis for such a link is uncertain (**Supplemental Appendix 3**). Clearly, more work is needed to elucidate the mechanism underlying ICL traverse.

Supplemental Material >

Given that similar X-shaped structures are formed during fork convergence and after traverse (compare **Figures 3*b***, **subpanel *ii*** and **3*c***, **subpanel *ii***), it has been proposed that the ICL is unhooked by essentially the same mechanism in both cases (77). Consistent with this idea, Lopes and colleagues (84) found that in the absence of SLX4 or XPF, but not MUS81, sister chromatids remained linked after traverse. Since traverse and fork convergence both appear to feed into the FA pathway, the balance between these two subpathways is of interest. While numerous genetic manipulations that impair traverse have little effect on the frequency of fork convergence (77), the elimination of PRIMPOL increases convergence to approximately 35% (85). This result suggests that traverse and convergence can compete. When adjacent ICLs are located between two pre-replication complexes (pre-RCs), or when an ICL is situated between the telomere and the last pre-RC, fork convergence cannot occur, and traverse is predicted to be essential for ICL repair. Conversely, convergence might be prioritized in cells with very short interorigin distances, as seen in the early frog embryo.

Does ICL Repair Normally Involve a One-Ended or Two-Ended Double-Strand Break?

The description of replication fork convergence in egg extracts triggered a debate about whether ICL repair is normally initiated by one or two forks (6, 54). With the subsequent discovery of traverse, which yields essentially the same X-shaped structure as fork convergence, the critical question has become whether ICL repair involves a one-ended DSB (**Figure 3*a***) or two-ended DSB (**Figure 3*b*,*c***). Several arguments have been advanced in favor of the former mechanism (6). First, because nonhomologous end joining (NHEJ) normally appears to play a minimal role in ICL repair (32, 86), ICL repair cannot involve a two-ended break. However, when an X-shaped structure is converted to a two-ended DSB, at least one of the DNA ends may contain a ssDNA overhang of sufficient length to preclude Ku binding and prevent NHEJ (34) (**Figure 3*b*,*c***). In addition, although it has been reported that, in the absence of the FA pathway, NHEJ is toxic (87, 88), other evidence shows that, in this setting, end joining helps overcome cross-linking agents, consistent with a two-ended break intermediate (89, 90). Second, DNA damage activates ATR signaling and globally inhibits origin firing, reducing the probability of fork convergence. However, while checkpoint signaling inhibits late origin firing, it stimulates activation of local dormant origins (91) and thus might actually stimulate fork convergence. Moreover, as discussed above, ATR signaling promotes traverse. Third, ICLs cause sister chromatid exchange (SCE) (19). The probability of SCE is higher after formation of a one-ended DSB (**Figure 3*a***, **subpanel *v***) than of a two-ended DSB because a DHJ can be dissolved without SCE (92) (**Figure 3*b***, **subpanels *vi–viii***). On this basis, it was inferred that ICL repair is usually triggered by single replication forks (6). However, although ICLs induce SCEs, in most instances these SCEs do not depend on the FA pathway (reviewed in 19, but see 29). We propose that the FA-independent SCEs caused by ICLs result from processing of the unrepaired lesions in mitosis by the same mechanism involved in common fragile site expression (**Supplemental Figure 1**). Notably, the lack of FA-dependent SCEs does not prove that repair is triggered by convergence or traverse, because after incision of a single fork (**Figure 3*a***), the arrival of a second fork could generate a two-ended DSB that is repaired without SCE formation. Thus, SCE data do not definitively argue in favor of the one-ended or two-ended DSB mechanism.

Supplemental Material >

In conclusion, current evidence does not distinguish between one- and two-ended DSB mechanisms. Nevertheless, we propose that the postreplicative mechanisms of fork convergence and traverse are more advantageous than a single fork mechanism. The drawback of triggering repair with a single fork is that it would be difficult to distinguish between fork arrest at an ICL versus

at transient barriers such as stable nucleoprotein complexes. As a result, a single fork mechanism would probably lead to unnecessary fork collapse and genome instability.

Recruitment of the Core Complex to Stressed Replication Forks

A critical question is how the FA core complex recognizes stressed replication forks and promotes ID ubiquitylation at these sites. Because ID and ID^{Ub} exhibit limited preference for structured DNAs (93–95), they cannot be responsible for sensing stalled forks. Instead, this function is encoded at least in part by the FANCM module, which interacts stably with the FA core complex through an interaction with FANCF (75) (see the dashed arrow in **Figure 4**). FANCM contains an

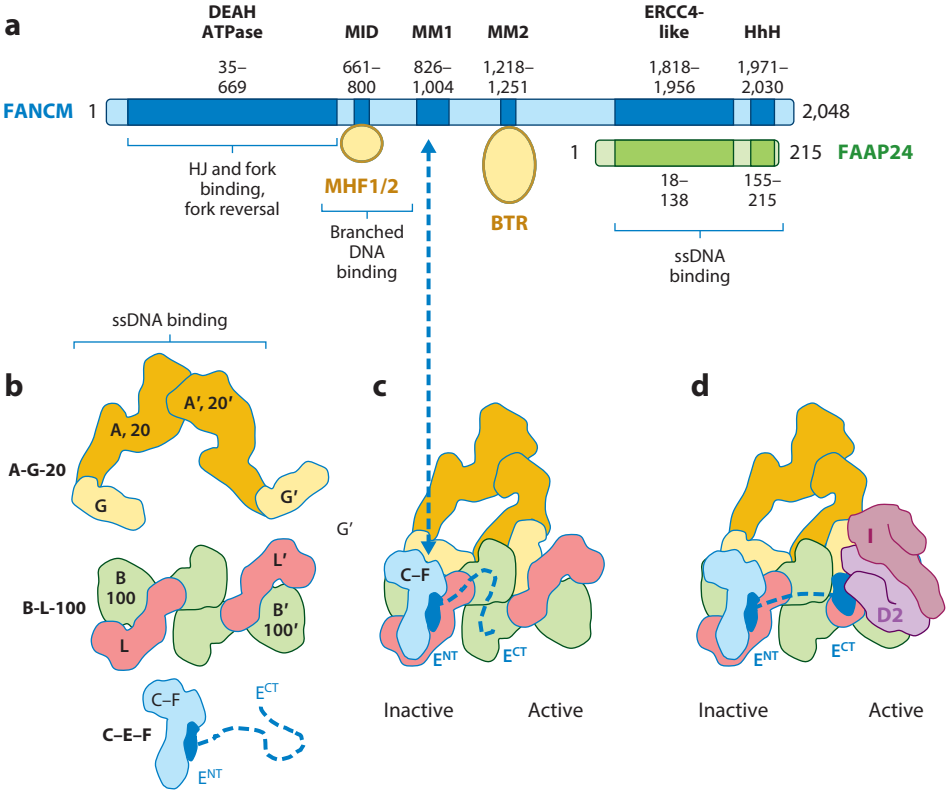

Figure 4

Schematic of the FANCM and FA core complexes. (*a*) The FANCM complex, showing the identity and location of key functional domains in FANCM and FAAP24, the proteins they bind, and DNA-binding activities associated with select domains. The ERCC4-like nuclease domains in FANCM and FAAP24 are inactive. The double-headed arrow indicates the interaction between MM1 of FANCM and FANCF of the core complex. (*b*) Schematic of the A-G-20, C-E-F, and B-L-100 complexes. The flexible linker between the N-terminal and C-terminal domains of FANC is illustrated as a dotted line. (*c*) Schematic of the entire FA core complex, including the asymmetric binding of A-G-20 to B-L-100, which allows only one C-E-F module to associate, establishing active and inactive sides of the complex. (*d*) Schematic of the FA core complex binding to unubiquitylated ID lacking DNA. Upon ID binding to the core complex, the C terminus of FANCE becomes ordered. Abbreviations: BTR, BLOOM-TOP3A-RMI1-RMI2; FA, Fanconi anemia; HhH, helix-hairpin-helix; HJ, Holliday junction; MID, MHF-interacting domain; MM1, FANCM motif 1; MM2, FANCM motif 2; ssDNA, single-stranded DNA.

N-terminal DEAH-type ATPase domain, an inactive nuclease fold at its C terminus that dimerizes with FAAP24 (96), and internal motifs that bind to FANCF, BTR, and the MHF1-MHF2 histone fold heterodimer, respectively (97) (**Figure 4*a***). Localization of the core complex to chromatin after DNA damage depends on FANCM, FAAP24, and MHF1 but is independent of FANCD2, FANCI, and FANCM ATPase activity (78, 98–101). Consistent with this, efficient FANCD2 ubiquitylation and ICL tolerance requires FANCM, FAAP24 (96), MHF1, and MHF2 (100, 102). The FANCM module contains at least three DNA-binding domains (**Figure 4*a***). First, using its N-terminal DEAH domain, FANCM binds and remodels replication forks and Holliday junctions (83, 103). Second, the C-terminus of FANCM complexed with FAAP24 binds preferentially to ssDNA (96). Third, when bound to a FANCM peptide, the MHF1-MHF2 histone fold complex prefers binding to a branched duplex DNA structure such as a Holliday junction (104, 105).

Importantly, diverse forms of replication stress, including ICLs, hydroxyurea, and ultraviolet light promote ID ubiquitylation (106–108). Therefore, the FANCM module must be able to detect different types of stressed forks. Most likely, the DEAH domain of FANCM binds to the branchpoint of the stalled fork, and the FAAP24 and MHF DNA-binding domains further stabilize the complex on DNA by interacting with the two arms of the fork (102, 104, 105), whether these both comprise ssDNA, as expected after HU exposure, or one contains dsDNA and the other ssDNA, as expected at ICLs (**Figure 3*b***, **subpanel *ii***). In addition to the DNA-binding activities of the FANCM module, FANCA of the core complex binds tightly to ssDNA and thus might also help recruit the core to chromatin (109). Consistent with independent roles for FANCM and FANCA in core complex recruitment, mutation of FANCM or FANCG [which tethers FANCA to the core complex (110)] causes a partial defect in core complex recruitment, whereas simultaneous deletion of FANCG and FANCM eliminates recruitment (111). Interestingly, some evidence indicates that MutSα contributes to chromatin recruitment of the core complex (112, 113), but the functional significance of this mechanism is unclear. A future challenge will be to understand how these multiple DNA-binding functionalities cooperate to recruit the core complex to diverse forms of replication stress. It will also be important to explore the role of chromatin in core complex recruitment, especially since the UBZ domain of FAAP20 has been proposed to bind ubiquitinated histones (114).

The Mechanism of ID Ubiquitylation by the Core Complex

Biochemical and genetic evidence have shown that the FA core complex consists of three subassemblies (111, 115) (**Figure 4*b***): FANCC-FANCE-FANCF (C-E-F), FANCA-FANCG-FAAP20 (A-G-20), and FANCB-FANCL-FAAP100 (B-L-100). B-L-100 is the catalytic module, with FANCL using its RING finger domain to bind the E2-conjugating enzyme FANCT (UBE2T), which transfers ubiquitin to ID (116, 117). Although FANCL and UBE2T are sufficient to ubiquitylate FANCD2 in the test tube, the presence of FANCB, FAAP100, and the C-E-F module greatly stimulates the reaction (115, 118). Consistent with the central role of B-L-100, deletions of FANCL, FANCB, or FAAP100 completely eliminate FANCD2 ubiquitylation in cells (111, 118). In contrast, mutations in C-E-F or A-G-20 drastically reduce but do not eliminate ubiquitylation, consistent with these modules helping to recruit ID and possibly to localize the core at stressed forks.

The FA core complex is built around a dimer of B-L-100 modules (115, 119, 120), which interacts with a dimer of A-G-20 modules (110) (**Figure 4*b,c***). Importantly, the symmetry of the core complex is broken because the FANCG subunits of the two A-G-20 modules interact with different surfaces of the two B-L-100 modules (110) (**Figure 4*c***). As a result, only one side of the core complex binds a C-E-F module (see the left side of **Figure 4*c***). Importantly, C-E-F blocks

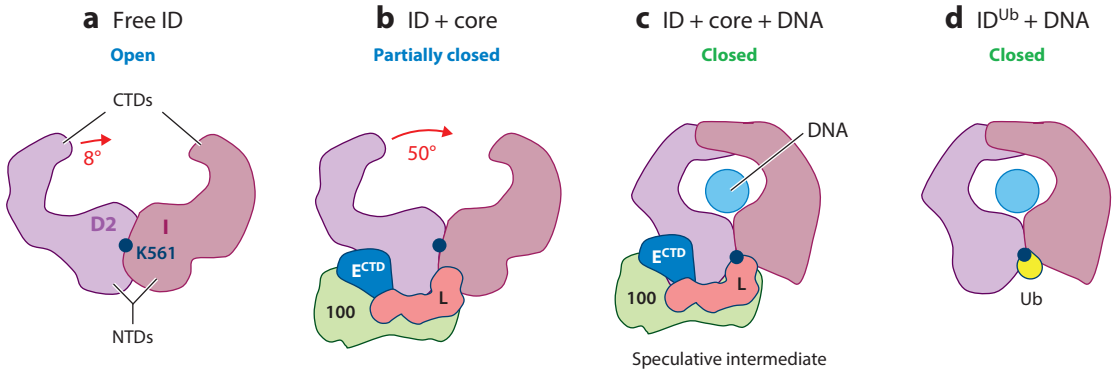

Figure 5

Mechanism of ID ubiquitylation. (*a*) In free ID, FANCI and FANCD2 interact via their NTDs. Ubiquitylation sites are buried within the NTD interface, and CTDs are far apart. The red arrow indicates the 8° movement of the CTDs toward each other upon binding of the FA core complex. (*b*) The FA core complex binds ID with the RING domain of FANCL reaching into the ID interface and the CTD of FANCE binding the outside surface of FANCD2's NTD. The red arrow indicates the additional 50° movement of the CTDs toward each other that is required to mimic the conformation of ID^{Ub}. (*c*) In a speculative intermediate step, DNA binding to ID closes the trough around DNA and exposes K561 for ubiquitylation. (*d*) Ubiquitylation on FANCD2 K561 locks ID into an open conformation and maintains FANCI K523 accessible for subsequent ubiquitylation (not shown). Abbreviations: CTD, C-terminal domain; FA, Fanconi anemia; ID^{Ub}, monoubiquitylated FANCI and FANCD2 heterodimer; NTD, N-terminal helical repeat domain.

the interaction of FANCL with ID, rendering one side of the core complex catalytically inactive. The absence of C-E-F on the other side enables FANCL to bind UBE2T and ID, rendering this side of the core catalytically active (see the right side of **Figure 4*d***). FANCE binds directly to FANCD2 and recruits it to the core complex (121). Interestingly, FANCE is anchored on the inactive side of the core via its N-terminal domain and contributes to ID recruitment on the active side via its C-terminal α-helical domain (122), which resides at the end of a long, flexible linker (**Figure 4*d***). Upon ID binding, the C-terminal domain of FANCE binds to ID and thus becomes ordered within the overall structure (**Figure 4*c,d***).

Together with the original ID structure (95), recent structures of the ID-FA core complex (110) and ID^{Ub} (93, 123) suggest a detailed mechanism of ID ubiquitylation. In the unmodified form, ID forms an open, trough-like structure in which the ubiquitylated lysines of both proteins are buried near the dimer interface, which is formed by the N-terminal helical repeat domains (NTDs) of each protein (**Figure 5*a***). When ID docks onto the FA core complex via interactions with FANCE and FANCL, FANCL's RING domain inserts into and partially pries open the ID dimer interface near the target lysines, causing the C-terminal domains of FANCI and FANCD2 to rotate toward each other by approximately 8°, which initiates closing of the trough (110) (**Figure 5*a,b***). However, the lysine residues are still buried, raising the question of how ID can be ubiquitylated. Strikingly, in ID^{Ub}, the C termini rotate toward each other by a further 50° and interact, closing the trough around the DNA (93, 123) (**Figure 5*d***). In this conformation, the lysines are fully exposed. A mutation in the CTD of FANCI that disrupts the interaction with FANCD2's CTD is less efficiently ubiquitylated and binds less tightly to DNA (23, 93, 124). Based on these observations, an attractive hypothesis is that DNA binding to the ID-FA core complex closes the trough and exposes the lysines for subsequent ubiquitylation (123) (**Figure 5*b,c***). Ubiquitylation thus locks the ID complex into a conformation that cannot release DNA. This model is consistent with prior evidence showing that DNA strongly stimulates ID ubiquitylation in vitro (118, 125) and that the ID complex binds chromatin in vivo before

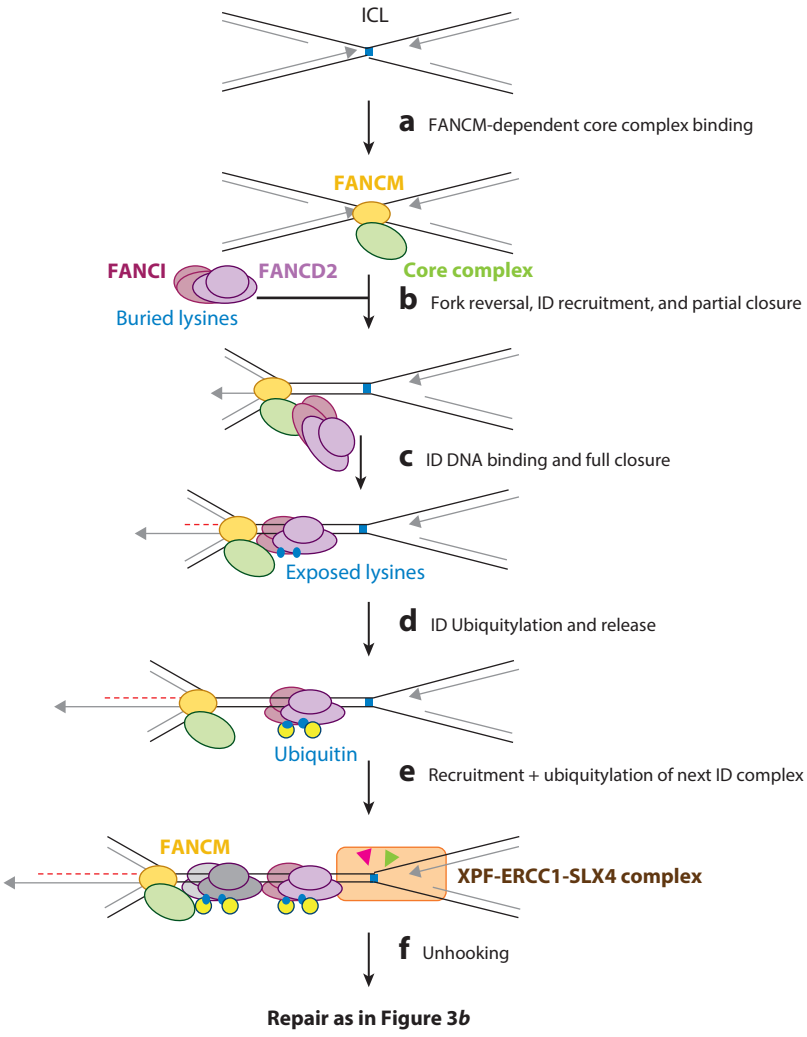

Figure 6

Mechanism and effects of ID ubiquitylation at a stressed replication fork. After FANCM-dependent core complex recruitment (*a*), fork reversal (*b*), and ID recruitment (*c*), ID undergoes closure (*d*) and ubiquitylation (*d*). Recruitment and ubiquitylation of additional ID complexes stabilize the reversed fork (*e*) and/or create a platform for XPF-dependent unhooking (*f*). Abbreviations: ICL, interstrand cross-link; Ub, ubiquitin.

undergoing ubiquitylation (126). Consistent with it forming a clamp around DNA, ID^{Ub} has a higher affinity for and a slower off rate from DNA than ID (93, 123, 124, 127). Together, these results suggest the following sequence of events at stressed forks. FANCM binds the stressed replication fork, bringing with it the core complex (**Figure 6*a***). The core complex recruits and partially closes the ID trough (**Figure 6*b***), whose subsequent interaction with DNA fully closes the trough, exposing K561 (**Figure 6*c***) and promoting FANCD2 ubiquitylation by the core complex (**Figure 6*d***). FANCD2 ubiquitylation in turn helps expose K523 in FANCI, allowing its subsequent ubiquitylation (110, 115). A crucial test of this model will be to address whether DNA binding to the ID-FA core complex closes the trough prior to ubiquitylation (**Figure 5*c***).

Supplemental Material >

ID ubiquitylation is subject to several forms of positive and negative regulation. Cellular exposure to ICLs leads to activation of the ATR checkpoint kinase via a poorly defined mechanism (**Supplemental Appendix 4**). ATR activity is required for FANCD2 ubiquitylation and suppression of ICL sensitivity (108). ATR phosphorylates FANCI at several sites along the FANCI-FANCD2 NTD interface and thereby might help promote closing of the ID clamp, exposing K561 and K523 for ubiquitylation (22, 95, 128). ID^{Ub} is deubiquitylated by Usp1 (129), whose activity depends on its dimerization partner UAF1 (130). FANCI ubiquitylation and ATR phosphorylation impairs FANCD2 deubiquitylation by USP1 and thus helps preserve ID^{Ub} (124, 128, 131). Strikingly, cells lacking Usp1 contain constitutively ubiquitylated FANCD2 and are sensitive to cross-linking agents (132, 133). These results raise the possibility that after ID^{Ub} performs its function, its clamp-like interaction with DNA is inhibitory for subsequent steps of repair, requiring ID^{Ub} removal. However, it cannot be ruled out that in the absence of USP1, constitutively ubiquitylated ID is sequestered on chromatin and unable to relocalize to ICLs where these arise. Interestingly, a fusion of FANCD2 and ubiquitin is partially functional, arguing against an absolute requirement for FANCD2 deubiquitylation in ICL repair (134). On the other hand, sumo-directed ubiquitylation and clearance of ID from sites of DNA damage by the p97 ATPase promotes cell survival in the face of ICLs, consistent with the possibility that ID^{Ub} removal from sites of damage contributes to repair (135).

The Role of ID^{Ub} in Repair

For years, it was widely assumed that ubiquitylated FANCD2 recruits one or more effectors of ICL repair. However, it is now clear that the hydrophobic patch (including residue I44) of the ubiquitin attached to FANCD2 is buried at the ID interface (93, 123). Therefore, canonical ubiquitin-binding motifs, which recognize I44 (136), cannot bind ubiquitin within ID^{Ub}. Indeed, a host of putative FA pathway effectors exhibit no preferential binding to ID^{Ub} compared to ID (127). Nevertheless, SLX4 recruitment to ICLs requires FANCD2 ubiquitylation in egg extracts (43), but whether this is true in mammalian cells is controversial (46, 47, 50). An updated model is that ID^{Ub} effectors such as SLX4-XPF bind the solvent-exposed surface of ubiquitin or interact with regions of DNA-bound ID^{Ub} that are distant from ubiquitin (**Figure 6*e***). An alternative but not mutually exclusive hypothesis is that ID^{Ub} promotes ICL repair indirectly by organizing local DNA or chromatin structure. For example, if FANCM promotes fork reversal at ICLs, as it travels away from the ICL, it might deposit multiple ID^{Ub} molecules in its wake, generating an ID^{Ub} array (127) (**Figure 6*e***). This would prevent fork restoration, allowing time for XPF-dependent incision of the ICL. If fork reversal is not integral to ICL repair, ID^{Ub} is probably deposited on one or more arms of the X-shaped structure surrounding the ICL, but how this would promote unhooking is unclear. In addition to its essential role in promoting incisions, ID^{Ub} also enhances homologous recombination via poorly defined mechanisms (**Supplemental Appendix 5**). In conclusion, how ID^{Ub} promotes ICL repair and how the clamping of ID^{Ub} on DNA relates to this function remains an enduring mystery of the FA pathway.

THE NEIL3 PATHWAY

To address whether different ICLs are repaired by different mechanisms, Semlow et al. (137) investigated repair of psoralen-ICLs and AP-ICLs in *Xenopus* egg extracts. Surprisingly, these lesions are not unhooked via incisions in the phosphodiester backbone, as seen in the FA pathway. Instead, they are resolved by the DNA glycosylase NEIL3, which cleaves one of the two *N*-glycosyl bonds that form the cross-link (**Figure 7**). Like the FA pathway, the NEIL3

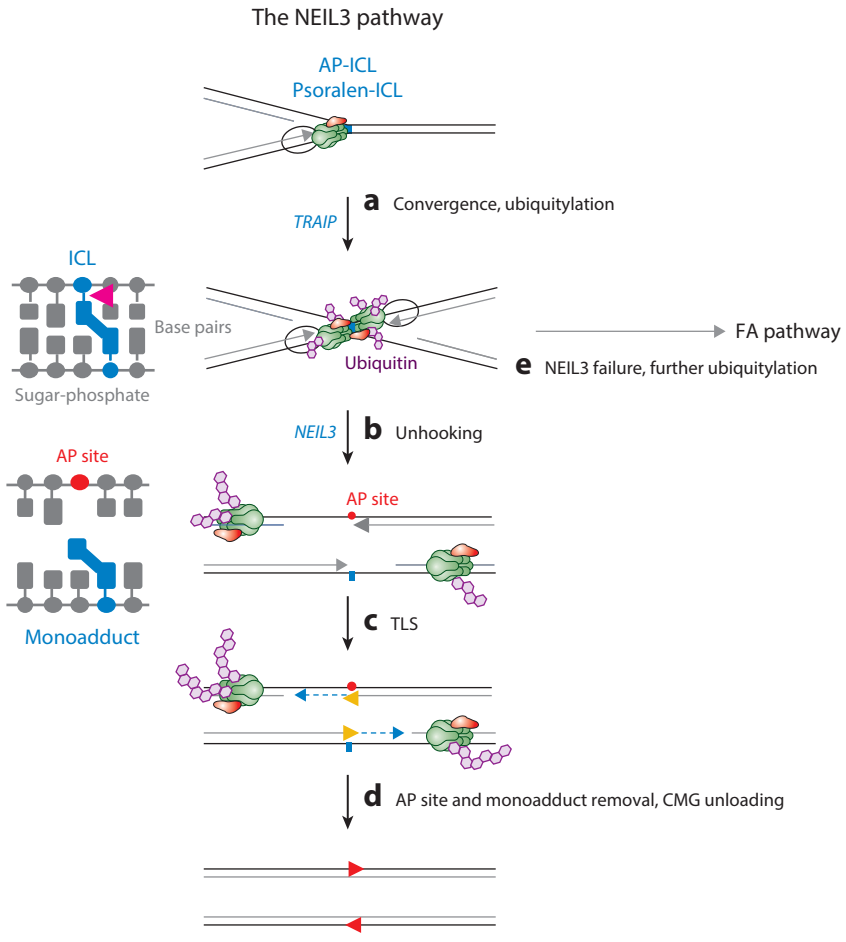

Figure 7

The NEIL3 pathway of ICL repair. The pink arrowhead illustrates NEIL3-dependent cleavage of one of the two glycosyl bonds that form the ICL, leaving an abasic (AP) site in one strand and a monoadduct in the other strand. Yellow arrowheads indicate the insertion of a nucleotide across from the AP site and monoadduct, respectively. Red arrowheads indicate the excision repair of an AP site and monoadduct (hypothetical). The green hexamer indicates CMG and the red oval TRAIP. In the case of AP-ICLs, NEIL3 action generates an AP site in one strand and a normal adenosine in the other strand (not shown). Abbreviations: AP, apurinic/apyrimidinic; ICL, interstrand cross-link; TLS, translesion synthesis.

pathway requires replication fork convergence at the ICL to activate TRAIP-dependent CMG ubiquitylation (**Figure 7*a***) and probably to place the lesion into an ssDNA context, which NEIL3 prefers (138). However, CMG unloading is not required for AP- or psoralen-ICL unhooking. Rather, CMG ubiquitylation recruits NEIL3 via the latter's NPL4-type zinc finger (NZF) ubiquitin-binding motif (36). In the case of psoralen ICLs, NEIL3 unhooking yields an AP site in one strand and a psoralen monoadduct in the other strand (**Figure 7*b***), both of which are bypassed using the DNA Pol ζ–Rev1 complex (**Figure 7*c***). In the case of AP-ICLs (**Figure 1**), NEIL3 reverses the ICL, regenerating a normal adenosine in one strand and an AP site in the other strand that is bypassed by TLS. The final steps of repair probably involve excision of the AP site and monoadduct. After ICL unhooking, CMG likely translocates onto dsDNA (**Figure 7*c***), from

which it is probably removed by the same pathway that operates during replication termination (139) (**Figure 7*d***). Although the NEIL3 pathway avoids a DSB intermediate, the production of an AP site virtually guarantees the generation of a point mutation. Importantly, cisplatin-ICLs are not processed by NEIL3, possibly because their distorted DNA structure (8) precludes the action of NEIL3 and thus requires the FA pathway, which incises DNA adjacent to the ICL.

Consistent with their relative complexities (**Figure 3*b*** versus **Figure 7**), the NEIL3 pathway is faster and more efficient than the FA pathway (137). This explains why psoralen- and AP-ICLs are unhooked almost exclusively by the NEIL3 pathway in extracts. However, in the absence of NEIL3, these lesions are funneled into the FA pathway (137), an effect also seen in mammalian cells (36, 38). This prioritization of the NEIL3 pathway is linked to CMG ubiquitylation (36). Thus, short ubiquitin chains are sufficient to recruit NEIL3, whereas longer chains are required to activate the p97 ATPase. In this manner, NEIL3 first gains access to the stalled CMGs, but if NEIL3 fails to cleave the ICL, as seen for cisplatin ICLs, the ubiquitin chains grow, leading to recruitment of p97, CMG unloading, and FA pathway activation (**Figure 7*e***). Together, the data establish NEIL3-dependent unhooking as a new mechanism of ICL repair that avoids DSB formation. Moreover, while NEIL3 is prioritized over the FA pathway, the latter is more versatile, as it appears able to unhook any ICL.

What are the endogenous lesions repaired by the NEIL3 pathway? Given that several thousand AP sites are present at steady state in mammalian cells (140), AP-ICLs are a good candidate, but this must be examined directly. Also, what is the consequence of a defective NEIL3 pathway? Like *FANC*$^{-/-}$ mice, *NEIL3*$^{-/-}$ mice do not recapitulate the human FA phenotype (141). Notably, a hypomorphic allele of *NEIL3* causes a human autoimmune disorder with no symptoms of FA (142). The absence of an FA phenotype could be due to residual glycosylase activity in the mutant protein or redundancy with the FA pathway. Thus, although NEIL3 might normally process the majority of certain lesions, the versatility of the FA pathway probably makes it more important for cell survival. Given that ICL traverse appears to predominate over fork convergence (77), why is NEIL3 recruitment coupled to CMG ubiquitylation, which requires fork convergence (137)? Perhaps NEIL3 can also be recruited independently of convergence in mammalian cells via the rapid, PARP-dependent mechanism recently identified (38). In conclusion, the NEIL3 pathway shows that ICLs can be unhooked in the absence of DSB formation, but its significance remains to be elucidated.

THE ACETALDEHYDE PATHWAY

Given the possible connection of acetaldehyde-induced ICLs (AA-ICLs) to the etiology of FA (**Supplemental Appendix 1**), it was of particular interest to determine how these lesions are repaired. Like all other ICLs tested so far, replication-coupled repair of AA-ICLs in egg extracts requires fork convergence (143) (**Figure 8*a***). However, while approximately 50% of these ICLs are incised by the FA pathway, the other half are unhooked without incisions (**Figure 8*b***). Surprisingly, AA-ICL unhooking does not involve NEIL3 or generate an abasic site, indicating it does not involve a DNA glycosylase. Instead, unhooking appears to regenerate an undamaged dG in one strand and a propanoguanine adduct in the other strand, from which the cross-link is initially formed (**Figure 1*f***). After unhooking, gap filling past the propanoguanine requires TLS. These results suggest that the cross-link undergoes enzymatic reversal, but the enzyme responsible has not been identified. Surprisingly, when the FA pathway is blocked, flux through the AA-ICL unhooking pathway does not increase, suggesting that after fork convergence, a fraction of lesions becomes irreversibly committed to the FA pathway. Alternatively, the AA-ICL repair pathway may not be able to process all three AA-ICL isoforms generated during synthesis (**Figure 1*f***).

Supplemental Material >

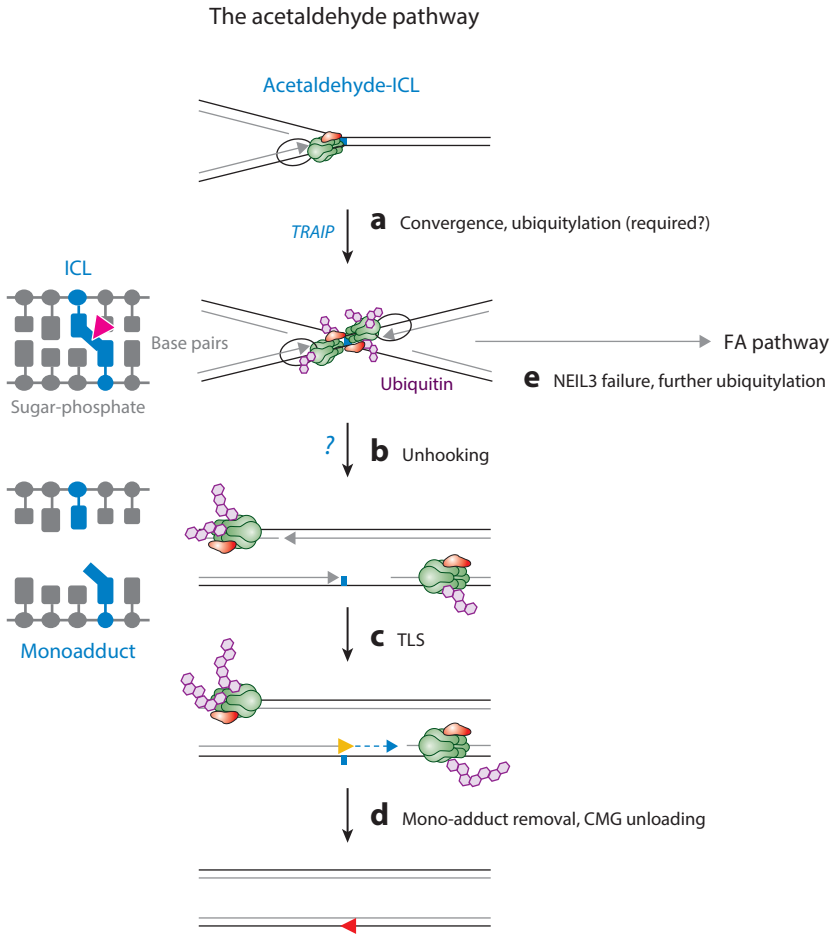

Figure 8

The AA pathway of ICL repair. The pink arrowhead illustrates cleavage in the middle of the AA-ICL by an unknown enzyme, which is predicted to create two monoadducts, both of which are bypassed by TLS (*yellow arrowheads*). Red arrowheads indicate excision repair of monoadducts (hypothetical). Abbreviations: AA, acetaldehyde; AP, apurinic/apyrimidinic; FA, Fanconi anemia; ICL, interstrand cross-link; TLS, translesion synthesis.

Whatever the underlying reason, the reliance on the FA pathway to process some AA-ICLs would explain why loss of the FA pathway causes human disease. The principle future challenge is to identify the putative AA-ICL unhooking enzyme and determine whether its loss causes an FA phenotype in humans.

REPLICATION-INDEPENDENT ICL REPAIR

While the loss of replication-coupled ICL repair, especially the FA pathway, causes extreme sensitivity to ICL-inducing agents, there is evidence that ICLs can also be sensed and repaired independently of replication. Such a mechanism is crucial in nondividing cells, especially when an ICL disrupts an essential gene. The logic of replication-independent interstrand cross-link repair (RIR) most closely resembles that of the FA pathway in that the ICL appears to be unhooked using

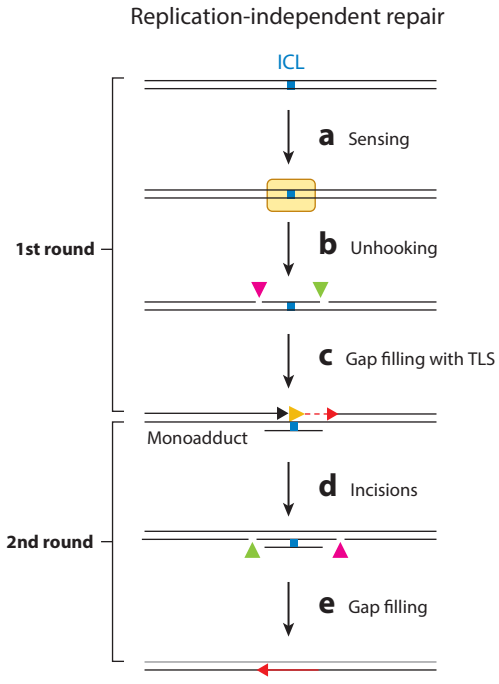

Figure 9

Mechanism of RIR. In bacteria, RIR involves two rounds of excision repair according to the following general steps (reviewed in 27, 144): (*a*) ICL sensing (ICL-sensing factor, *tan square*); (*b*) dual incisions (*pink* and *green arrowheads*) in one strand that unhook the ICL and leave behind a remnant (monoadduct) of the ICL attached to the other strand; (*c*) strand extension past the monoadduct using a translesion DNA polymerase (*yellow* and *red arrows*) or homologous recombination (not depicted); (*d*) dual incisions (*pink* and *green arrowheads*) to remove the remaining monoadduct via a second round of incisions; and (*e*) a second round of gap filling (*red arrow*). Abbreviations: ICL, interstrand cross-link; RIR, replication-independent interstrand cross-link repair; TLS, translesion synthesis.

nucleolytic incisions. In bacteria, RIR involves two rounds of excision repair (reviewed in 27, 144) (**Figure 9**). Evidence suggests that a similar mechanism of RIR operates in yeast and vertebrates with possible modifications (reviewed in 7, 27). In mammalian cells, ICLs are sensed by the nucleotide excision repair protein XPC, and at least one incision is performed by XPF-ERCC1, as seen in the FA pathway. Interestingly, in mammalian cell extracts, ICLs induce dual incisions by the nucleotide excision repair pathway, but both incisions occur on the 5′ side of the ICL (145). An attractive model is that the 5′ gap provides an entry point for a 5′ to 3′ exonuclease that degrades DNA past the ICL (145). As in the FA pathway, SNM1A and FAN1 are excellent candidates for such a nuclease. Consistent with the involvement of SNM1A and FAN1 in RIR, both genes exhibit nonepistasis with the FA pathway (60, 146). Once the ICL has been unhooked, subsequent gap filling involves the TLS enzyme Pol ζ (62) (**Figure 2*c***). During RIR in *Xenopus* egg extracts, lesion recognition and at least one incision are reported to involve the MMR factors MutSα and MutLα, respectively (147), and TLS involves DNA polymerase κ (148). However, activation of MutLα during replication to remove mismatches usually involves a strand discontinuity, and it is unclear how such a signal would be generated at an ICL. Thus, both ICL detection and sensing during RIR remain to be fully elucidated.

Importantly, vertebrate RIR is greatly enhanced on ICLs that induce distortions in the double helix, presumably because these can be detected by XPC and/or MutSα independently of replication (147, 149). However, repair of nondistorting lesions can be triggered through collision with an RNA polymerase (150). As seen for transcription-coupled nucleotide excision repair (151), transcription-coupled ICL repair involves the Cockayne syndrome proteins CSA and CSB. How these proteins couple RNAPII pausing to ICL repair is unclear, but one possibility is the direct recruitment of the SNM1A nuclease (152). In summary, RIR represents an important mode of ICL repair that not only removes ICLs in nonproliferating cells but also reduces the ICL burden before dividing cells enter S phase (150).

SYNOPSIS OF ICL REPAIR PATHWAY CHOICE

Three factors likely dominate ICL repair pathway choice. The first is the chemistry of the cross-link. ICLs that are highly distorting are recognized independently of DNA replication and can be removed in G1 or G2. Conversely, ICLs that do not significantly distort the double helix are not recognized until they block replication fork progression. Further, the structure of the ICL dictates which replication-dependent pathway acts on the lesion. The second factor involves timing. Even a highly distorting ICL will be processed by replication-coupled repair if it is generated in S phase, right before passage of a DNA replication fork. Finally, the location of ICLs determines their fate. ICLs located in highly transcribed regions are expected to be processed by transcription-coupled repair even if the lesions are nondistorting. Furthermore, it is possible that specific chromatin structures favor specific ICL repair pathways.

CONCLUSION

We now appreciate that vertebrates enlist at least five distinct mechanism to resolve ICLs (two replication-independent and three replication-coupled pathways). The RIR and FA pathways are related, because invariably the 5′ incision appears to be carried out by XPF-ERCC1. Moreover, in all cases, the 3′ incision might involve 5′ to 3′ exonuclease activity past the ICL using FAN1 and/or SNM1A. A future challenge is to develop robust cell-free systems of RIR, especially the transcription-coupled form, which is essential for a thorough understanding of this mechanism. Unexpectedly, the NEIL3 and acetaldehyde pathways unhook ICLs by fundamentally distinct mechanisms that avoid incisions and DSB formation. These pathways are prioritized over the FA pathway and probably resolve the majority of certain ICLs. However, the FA pathway, being able to act on any ICL, appears to be the most important for suppressing genome instability and human disease. It will be important to test the prediction that the incision-independent pathways generate point mutations but fewer gross chromosomal rearrangements than does the FA pathway. Another important goal is to experimentally manipulate the balance between these various repair pathways. Upregulating a non-FA repair pathway, or changing its specificity to operate on ICLs normally targeted by the FA mechanism, might ameliorate the symptoms of FA. Conversely, targeted downregulation of ICL repair can induce synthetic lethality, as seen for NEIL3 and FA (36) or FAN1 and SNM1A (60). Combined with the right chemotherapy agent, inhibition of NEIL3 could be used to target BRCA1 and BRCA2 tumors that are deficient in the FA pathway. The ultimate goal of DNA repair studies is to elucidate mechanisms at the molecular level. In this regard, the structural elucidation of the FA core complex and ID^{Ub} is a spectacular advance that will surely transform research into the FA pathway. One can only hope that similar advances in the structural understanding of other ICL repair pathways will soon follow.

DISCLOSURE STATEMENT

J.C.W. is a cofounder of MoMa Therapeutics, in which he has a financial interest.

ACKNOWLEDGMENTS

We apologize to colleagues whose papers we could not discuss due to space limitations. We thank Michael Seidman, Alex Wu, and Ravi Amunugama for helpful discussions and feedback. Work on ICL repair in J.C.W.'s laboratory is supported by R01HL098316. J.C.W. is an American Cancer Society Research Professor and an investigator of the Howard Hughes Medical Institute.

LITERATURE CITED

1. Lawley PD, Phillips DH. 1996. DNA adducts from chemotherapeutic agents. *Mutat. Res.* 355:13–40
2. Brookes P, Lawley PD. 1960. The reaction of mustard gas with nucleic acids in vitro and in vivo. *Biochem. J.* 77:478–84
3. Deans AJ, West SC. 2011. DNA interstrand crosslink repair and cancer. *Nat. Rev. Cancer* 11:467–80
4. Niraj J, Farkkila A, D'Andrea AD. 2019. The Fanconi anemia pathway in cancer. *Annu. Rev. Cancer Biol.* 3:457–78
5. Gates KS. 2009. An overview of chemical processes that damage cellular DNA: spontaneous hydrolysis, alkylation, and reactions with radicals. *Chem. Res. Toxicol.* 22:1747–60
6. Legerski RJ. 2010. Repair of DNA interstrand cross-links during S phase of the mammalian cell cycle. *Environ. Mol. Mutagen.* 51:540–51
7. Williams HL, Gottesman ME, Gautier J. 2013. The differences between ICL repair during and outside of S phase. *Trends Biochem. Sci.* 38:386–93
8. Huang H, Zhu L, Reid BR, Drobny GP, Hopkins PB. 1995. Solution structure of a cisplatin-induced DNA interstrand cross-link. *Science* 270:1842–45
9. Huang H, Hopkins PB. 1993. DNA interstrand cross-linking by formaldehyde: nucleotide sequence preference and covalent structure of the predominant cross-link formed in synthetic oligonucleotides. *J. Am. Chem. Soc.* 115:9401–8
10. Lu K, Collins LB, Ru H, Bermudez E, Swenberg JA. 2010. Distribution of DNA adducts caused by inhaled formaldehyde is consistent with induction of nasal carcinoma but not leukemia. *Toxicol. Sci.* 116:441–51
11. Hata T, Hoshi T, Kanamori K, Matsumae A, Sano Y, Shima T, Sugawara R. 1956. Mitomycin, a new antibiotic from *Streptomyces*. I. *J. Antibiot.* 9:141–46
12. Hata T, Koga F, Sano Y, Kanamori K, Matsumae A, et al. 1954. Carzinophilin, a new tumor inhibitory substance produced by *Streptomyces*. I. *J. Antibiot.* 7:107–12
13. Xue M, Kim CS, Healy AR, Wernke KM, Wang Z, et al. 2019. Structure elucidation of colibactin and its DNA cross-links. *Science* 365:eaax2685
14. Wilson MR, Jiang Y, Villalta PW, Stornetta A, Boudreau PD, et al. 2019. The human gut bacterial genotoxin colibactin alkylates DNA. *Science* 363:eaar7785
15. Xue M, Wernke KM, Herzon SB. 2020. Depurination of colibactin-derived interstrand cross-links. *Biochemistry* 59:892–900
16. Burgers PMJ, Kunkel TA. 2017. Eukaryotic DNA replication fork. *Annu. Rev. Biochem.* 86:417–38
17. Kottemann MC, Smogorzewska A. 2013. Fanconi anaemia and the repair of Watson and Crick DNA crosslinks. *Nature* 493:356–63
18. Auerbach AD. 2009. Fanconi anemia and its diagnosis. *Mutat. Res.* 668:4–10
19. Thompson LH, Hinz JM. 2009. Cellular and molecular consequences of defective Fanconi anemia proteins in replication-coupled DNA repair: mechanistic insights. *Mutat. Res.* 668:54–72
20. Duxin JP, Walter JC. 2015. What is the DNA repair defect underlying Fanconi anemia? *Curr. Opin. Cell Biol.* 37:49–60
21. Basbous J, Constantinou A. 2019. A tumor suppressive DNA translocase named FANCM. *Crit. Rev. Biochem. Mol. Biol.* 54:27–40

22. Ishiai M, Kitao H, Smogorzewska A, Tomida J, Kinomura A, et al. 2008. FANCI phosphorylation functions as a molecular switch to turn on the Fanconi anemia pathway. *Nat. Struct. Mol. Biol.* 15:1138–46
23. Smogorzewska A, Matsuoka S, Vinciguerra P, McDonald ER 3rd, Hurov KE, et al. 2007. Identification of the FANCI protein, a monoubiquitinated FANCD2 paralog required for DNA repair. *Cell* 129:289–301
24. Taniguchi T, Garcia-Higuera I, Andreassen PR, Gregory RC, Grompe M, D'Andrea AD. 2002. S-phase-specific interaction of the Fanconi anemia protein, FANCD2, with BRCA1 and RAD51. *Blood* 100:2414–20
25. Peng M, Litman R, Jin Z, Fong G, Cantor SB. 2006. BACH1 is a DNA repair protein supporting BRCA1 damage response. *Oncogene* 25:2245–53
26. Elia AE, Wang DC, Willis NA, Boardman AP, Hajdu I, et al. 2015. RFWD3-dependent ubiquitination of RPA regulates repair at stalled replication forks. *Mol. Cell* 60:280–93
27. Muniandy PA, Liu J, Majumdar A, Liu ST, Seidman MM. 2010. DNA interstrand crosslink repair in mammalian cells: step by step. *Crit. Rev. Biochem. Mol. Biol.* 45:23–49
28. Howlett NG, Taniguchi T, Olson S, Cox B, Waisfisz Q, et al. 2002. Biallelic inactivation of BRCA2 in Fanconi anemia. *Science* 297:606–9
29. Niedzwiedz W, Mosedale G, Johnson M, Ong CY, Pace P, Patel KJ. 2004. The Fanconi anaemia gene *FANCC* promotes homologous recombination and error-prone DNA repair. *Mol. Cell* 15:607–20
30. Mirchandani KD, McCaffrey RM, D'Andrea AD. 2008. The Fanconi anemia core complex is required for efficient point mutagenesis and Rev1 foci assembly. *DNA Repair* 7:902–11
31. Papadopoulo D, Guillouf C, Mohrenweiser H, Moustacchi E. 1990. Hypomutability in Fanconi anemia cells is associated with increased deletion frequency at the HPRT locus. *PNAS* 87:8383–87
32. De Silva IU, McHugh PJ, Clingen PH, Hartley JA. 2000. Defining the roles of nucleotide excision repair and recombination in the repair of DNA interstrand cross-links in mammalian cells. *Mol. Cell. Biol.* 20:7980–90
33. Niedernhofer LJ, Lalai AS, Hoeijmakers JH. 2005. Fanconi anemia (cross)linked to DNA repair. *Cell* 123:1191–98
34. Raschle M, Knipsheer P, Enoiu M, Angelov T, Sun J, et al. 2008. Mechanism of replication-coupled DNA interstrand crosslink repair. *Cell* 134:969–80
35. Zhang J, Dewar JM, Budzowska M, Motnenko A, Cohn MA, Walter JC. 2015. DNA interstrand cross-link repair requires replication-fork convergence. *Nat. Struct. Mol. Biol.* 22:242–47
36. Wu RA, Semlow DR, Kamimae-Lanning AN, Kochenova OV, Chistol G, et al. 2019. TRAIP is a master regulator of DNA interstrand crosslink repair. *Nature* 567:267–72
37. Hoffmann S, Smedegaard S, Nakamura K, Mortuza GB, Raschle M, et al. 2016. TRAIP is a PCNA-binding ubiquitin ligase that protects genome stability after replication stress. *J. Cell Biol.* 212:63–75
38. Li N, Wang J, Wallace SS, Chen J, Zhou J, D'Andrea AD. 2020. Cooperation of the NEIL3 and Fanconi anemia/BRCA pathways in interstrand crosslink repair. *Nucleic Acids Res.* 48:3014–28
39. Olivieri M, Cho T, Alvarez-Quilon A, Li K, Schellenberg MJ, et al. 2020. A genetic map of the response to DNA damage in human cells. *Cell* 182:481–96.e21
40. Fullbright G, Rycenga HB, Gruber JD, Long DT. 2016. p97 promotes a conserved mechanism of helicase unloading during DNA cross-link repair. *Mol. Cell. Biol.* 36:2983–94
41. Amunugama R, Willcox S, Wu A, Abdullah UB, El-Sagheer AH, et al. 2018. Replication fork reversal during DNA interstrand crosslink repair requires CMG unloading. *Cell Rep.* 23:3419–28
42. Gari K, Decaillet C, Delannoy M, Wu L, Constantinou A. 2008. Remodeling of DNA replication structures by the branch point translocase FANCM. *PNAS* 105:16107–12
43. Klein Douwel D, Boonen RA, Long DT, Szypowska AA, Raschle M, et al. 2014. XPF-ERCC1 acts in unhooking DNA interstrand crosslinks in cooperation with FANCD2 and FANCP/SLX4. *Mol. Cell* 54:460–71
44. Long DT, Joukov V, Budzowska M, Walter JC. 2014. BRCA1 promotes unloading of the CMG helicase from a stalled DNA replication fork. *Mol. Cell* 56:174–85
45. Knipscheer P, Raschle M, Smogorzewska A, Enoiu M, Ho TV, et al. 2009. The Fanconi anemia pathway promotes replication-dependent DNA interstrand cross-link repair. *Science* 326:1698–701

46. Lachaud C, Castor D, Hain K, Munoz I, Wilson J, et al. 2014. Distinct functional roles for the two SLX4 ubiquitin-binding UBZ domains mutated in Fanconi anemia. *J. Cell Sci.* 127:2811–17
47. Yamamoto KN, Kobayashi S, Tsuda M, Kurumizaka H, Takata M, et al. 2011. Involvement of SLX4 in interstrand cross-link repair is regulated by the Fanconi anemia pathway. *PNAS* 108:6492–96
48. Hoogenboom WS, Boonen R, Knipscheer P. 2019. The role of SLX4 and its associated nucleases in DNA interstrand crosslink repair. *Nucleic Acids Res.* 47:2377–88
49. Guervilly JH, Takedachi A, Naim V, Scaglione S, Chawhan C, et al. 2015. The SLX4 complex is a SUMO E3 ligase that impacts on replication stress outcome and genome stability. *Mol. Cell* 57:123–37
50. Kim Y, Spitz GS, Veturi U, Lach FP, Auerbach AD, Smogorzewska A. 2013. Regulation of multiple DNA repair pathways by the Fanconi anemia protein SLX4. *Blood* 121:54–63
51. Hashimoto K, Wada K, Matsumoto K, Moriya M. 2015. Physical interaction between SLX4 (FANCP) and XPF (FANCQ) proteins and biological consequences of interaction-defective missense mutations. *DNA Repair* 35:48–54
52. Crossan GP, van der Weyden L, Rosado IV, Langevin F, Gaillard PH, et al. 2011. Disruption of mouse Slx4, a regulator of structure-specific nucleases, phenocopies Fanconi anemia. *Nat. Genet.* 43:147–52
53. Abdullah UB, McGouran JF, Brolih S, Ptchelkine D, El-Sagheer AH, et al. 2017. RPA activates the XPF-ERCC1 endonuclease to initiate processing of DNA interstrand crosslinks. *EMBO J.* 36:2047–60
54. Zhang J, Walter JC. 2014. Mechanism and regulation of incisions during DNA interstrand cross-link repair. *DNA Repair* 19:135–42
55. Hodskinson MR, Silhan J, Crossan GP, Garaycoechea JI, Mukherjee S, et al. 2014. Mouse SLX4 is a tumor suppressor that stimulates the activity of the nuclease XPF-ERCC1 in DNA crosslink repair. *Mol. Cell* 54:472–84
56. Kuraoka I, Kobertz WR, Ariza RR, Biggerstaff M, Essigmann JM, Wood RD. 2000. Repair of an interstrand DNA cross-link initiated by ERCC1-XPF repair/recombination nuclease. *J. Biol. Chem.* 275:26632–36
57. Fisher LA, Bessho M, Bessho T. 2008. Processing of a psoralen DNA interstrand cross-link by XPF-ERCC1 complex in vitro. *J. Biol. Chem.* 283:1275–81
58. Wang AT, Sengerova B, Cattell E, Inagawa T, Hartley JM, et al. 2011. Human SNM1A and XPF-ERCC1 collaborate to initiate DNA interstrand cross-link repair. *Genes Dev.* 25:1859–70
59. Dronkert ML, de Wit J, Boeve M, Vasconcelos ML, van Steeg H, et al. 2000. Disruption of mouse SNM1 causes increased sensitivity to the DNA interstrand cross-linking agent mitomycin C. *Mol. Cell. Biol.* 20:4553–61
60. Thongthip S, Bellani M, Gregg SQ, Sridhar S, Conti BA, et al. 2016. *Fan1* deficiency results in DNA interstrand cross-link repair defects, enhanced tissue karyomegaly, and organ dysfunction. *Genes Dev.* 30:645–59
61. Fontebasso Y, Etheridge TJ, Oliver AW, Murray JM, Carr AM. 2013. The conserved Fanconi anemia nuclease Fan1 and the SUMO E3 ligase Pli1 act in two novel Pso2-independent pathways of DNA interstrand crosslink repair in yeast. *DNA Repair* 12:1011–23
62. Roy U, Scharer OD. 2016. Involvement of translesion synthesis DNA polymerases in DNA interstrand crosslink repair. *DNA Repair* 44:33–41
63. Budzowska M, Graham TG, Sobeck A, Waga S, Walter JC. 2015. Regulation of the Rev1-pol ζ complex during bypass of a DNA interstrand cross-link. *EMBO J.* 34:1971–85
64. Kim H, Yang K, Dejsuphong D, D'Andrea AD. 2012. Regulation of Rev1 by the Fanconi anemia core complex. *Nat. Struct. Mol. Biol.* 19:164–70
65. Berti M, Chaudhuri AR, Thangavel S, Gomathinayagam S, Kenig S, et al. 2013. Human RECQ1 promotes restart of replication forks reversed by DNA topoisomerase I inhibition. *Nat. Struct. Mol. Biol.* 20:347–54
66. Long DT, Raschle M, Joukov V, Walter JC. 2011. Mechanism of RAD51-dependent DNA interstrand cross-link repair. *Science* 333:84–87
67. Kim H, D'Andrea AD. 2012. Regulation of DNA cross-link repair by the Fanconi anemia/BRCA pathway. *Genes Dev.* 26:1393–408

68. Karanja KK, Cox SW, Duxin JP, Stewart SA, Campbell JL. 2012. DNA2 and EXO1 in replication-coupled, homology-directed repair and in the interplay between HDR and the FA/BRCA network. *Cell Cycle* 11:3983–96
69. Cheng WH, Kusumoto R, Opresko PL, Sui X, Huang S, et al. 2006. Collaboration of Werner syndrome protein and BRCA1 in cellular responses to DNA interstrand cross-links. *Nucleic Acids Res.* 34:2751–60
70. Karanja KK, Lee EH, Hendrickson EA, Campbell JL. 2014. Preventing over-resection by DNA2 helicase/nuclease suppresses repair defects in Fanconi anemia cells. *Cell Cycle* 13:1540–50
71. Rickman KA, Noonan RJ, Lach FP, Sridhar S, Wang AT, et al. 2020. Distinct roles of BRCA2 in replication fork protection in response to hydroxyurea and DNA interstrand cross-links. *Genes Dev.* 34:832–46
72. Wang AT, Kim T, Wagner JE, Conti BA, Lach FP, et al. 2015. A dominant mutation in human RAD51 reveals its function in DNA interstrand crosslink repair independent of homologous recombination. *Mol. Cell* 59:478–90
73. Shiraishi Y, Sandberg AA. 1978. Effects of mitomycin C on sister chromatid exchange in normal and Bloom's syndrome cells. *Mutat. Res.* 49:233–38
74. Hirano S, Yamamoto K, Ishiai M, Yamazoe M, Seki M, et al. 2005. Functional relationships of FANCC to homologous recombination, translesion synthesis, and BLM. *EMBO J.* 24:418–27
75. Deans AJ, West SC. 2009. FANCM connects the genome instability disorders Bloom's syndrome and Fanconi anemia. *Mol. Cell* 36:943–53
76. Berezney R, Dubey DD, Huberman JA. 2000. Heterogeneity of eukaryotic replicons, replicon clusters, and replication foci. *Chromosoma* 108:471–84
77. Huang J, Liu S, Bellani MA, Thazhathveetil AK, Ling C, et al. 2013. The DNA translocase FANCM/MHF promotes replication traverse of DNA interstrand crosslinks. *Mol. Cell* 52:434–46
78. Ling C, Huang J, Yan Z, Li Y, Ohzeki M, et al. 2016. Bloom syndrome complex promotes FANCM recruitment to stalled replication forks and facilitates both repair and traverse of DNA interstrand crosslinks. *Cell Discov.* 2:16047
79. Huang J, Zhang J, Bellani MA, Pokharel D, Gichimu J, et al. 2019. Remodeling of interstrand crosslink proximal replisomes is dependent on ATR, FANCM, and FANCD2. *Cell Rep.* 27:1794–808.e5
80. Sparks JL, Chistol G, Gao AO, Raschle M, Larsen NB, et al. 2019. The CMG helicase bypasses DNA-protein cross-links to facilitate their repair. *Cell* 176:167–81.e21
81. Wasserman MR, Schauer GD, O'Donnell ME, Liu S. 2019. Replication fork activation is enabled by a single-stranded DNA gate in CMG helicase. *Cell* 178:600–11.e16
82. Huang M, Kim JM, Shiotani B, Yang K, Zou L, D'Andrea AD. 2010. The FANCM/FAAP24 complex is required for the DNA interstrand crosslink-induced checkpoint response. *Mol. Cell* 39:259–68
83. Xue Y, Li Y, Guo R, Ling C, Wang W. 2008. FANCM of the Fanconi anemia core complex is required for both monoubiquitination and DNA repair. *Hum. Mol. Genet.* 17:1641–52
84. Mutreja K, Krietsch J, Hess J, Ursich S, Berti M, et al. 2018. ATR-mediated global fork slowing and reversal assist fork traverse and prevent chromosomal breakage at DNA interstrand cross-links. *Cell Rep.* 24:2629–42.e5
85. Gonzalez-Acosta D, Blanco-Romero E, Mutreja K, Llanos S, Miguez S, et al. 2020. PrimPol primase mediates replication traverse of DNA interstrand crosslinks. bioRxiv 2020.05.19.104729. **https://doi.org/10.1101/2020.05.19.104729**
86. Muller C, Calsou P, Salles B. 2000. The activity of the DNA-dependent protein kinase (DNA-PK) complex is determinant in the cellular response to nitrogen mustards. *Biochimie* 82:25–28
87. Adamo A, Collis SJ, Adelman CA, Silva N, Horejsi Z, et al. 2010. Preventing nonhomologous end joining suppresses DNA repair defects of Fanconi anemia. *Mol. Cell* 39:25–35
88. Pace P, Mosedale G, Hodskinson MR, Rosado IV, Sivasubramaniam M, Patel KJ. 2010. Ku70 corrupts DNA repair in the absence of the Fanconi anemia pathway. *Science* 329:219–23
89. Bunting SF, Callen E, Kozak ML, Kim JM, Wong N, et al. 2012. BRCA1 functions independently of homologous recombination in DNA interstrand crosslink repair. *Mol. Cell* 46:125–35
90. Garaycoechea JI, Crossan GP, Langevin F, Mulderrig L, Louzada S, et al. 2018. Alcohol and endogenous aldehydes damage chromosomes and mutate stem cells. *Nature* 553:171–77
91. Moiseeva TN, Bakkenist CJ. 2019. Dormant origin signaling during unperturbed replication. *DNA Repair* 81:102655

92. Bizard AH, Hickson ID. 2014. The dissolution of double Holliday junctions. *Cold Spring Harb. Perspect. Biol.* 6:a016477
93. Wang R, Wang S, Dhar A, Peralta C, Pavletich NP. 2020. DNA clamp function of the monoubiquitinated Fanconi anaemia ID complex. *Nature* 580:278–82
94. Yuan F, El Hokayem J, Zhou W, Zhang Y. 2009. FANCI protein binds to DNA and interacts with FANCD2 to recognize branched structures. *J. Biol. Chem.* 284:24443–52
95. Joo W, Xu G, Persky NS, Smogorzewska A, Rudge DG, et al. 2011. Structure of the FANCI-FANCD2 complex: insights into the Fanconi anemia DNA repair pathway. *Science* 333:312–16
96. Ciccia A, Ling C, Coulthard R, Yan Z, Xue Y, et al. 2007. Identification of FAAP24, a Fanconi anemia core complex protein that interacts with FANCM. *Mol. Cell* 25:331–43
97. Tao Y, Jin C, Li X, Qi S, Chu L, et al. 2012. The structure of the FANCM-MHF complex reveals physical features for functional assembly. *Nat. Commun.* 3:782
98. Kim JM, Kee Y, Gurtan A, D'Andrea AD. 2008. Cell cycle-dependent chromatin loading of the Fanconi anemia core complex by FANCM/FAAP24. *Blood* 111:5215–22
99. Mosedale G, Niedzwiedz W, Alpi A, Perrina F, Pereira-Leal JB, et al. 2005. The vertebrate Hef ortholog is a component of the Fanconi anemia tumor-suppressor pathway. *Nat. Struct. Mol. Biol.* 12:763–71
100. Singh TR, Saro D, Ali AM, Zheng XF, Du CH, et al. 2010. MHF1-MHF2, a histone-fold-containing protein complex, participates in the Fanconi anemia pathway via FANCM. *Mol. Cell* 37:879–86
101. Wang Y, Leung JW, Jiang Y, Lowery MG, Do H, et al. 2013. FANCM and FAAP24 maintain genome stability via cooperative as well as unique functions. *Mol. Cell* 49:997–1009
102. Yan Z, Delannoy M, Ling C, Daee D, Osman F, et al. 2010. A histone-fold complex and FANCM form a conserved DNA-remodeling complex to maintain genome stability. *Mol. Cell* 37:865–78
103. Gari K, Decaillet C, Stasiak AZ, Stasiak A, Constantinou A. 2008. The Fanconi anemia protein FANCM can promote branch migration of Holliday junctions and replication forks. *Mol. Cell* 29:141–48
104. Zhao Q, Saro D, Sachpatzidis A, Singh TR, Schlingman D, et al. 2014. The MHF complex senses branched DNA by binding a pair of crossover DNA duplexes. *Nat. Commun.* 5:2987
105. Fox D 3rd, Yan Z, Ling C, Zhao Y, Lee DY, et al. 2014. The histone-fold complex MHF is remodeled by FANCM to recognize branched DNA and protect genome stability. *Cell Res.* 24:560–75
106. Garcia-Higuera I, Taniguchi T, Ganesan S, Meyn MS, Timmers C, et al. 2001. Interaction of the Fanconi anemia proteins and BRCA1 in a common pathway. *Mol. Cell* 7:249–62
107. Howlett NG, Taniguchi T, Durkin SG, D'Andrea AD, Glover TW. 2005. The Fanconi anemia pathway is required for the DNA replication stress response and for the regulation of common fragile site stability. *Hum. Mol. Genet.* 14:693–701
108. Andreassen PR, D'Andrea AD, Taniguchi T. 2004. ATR couples FANCD2 monoubiquitination to the DNA-damage response. *Genes Dev.* 18:1958–63
109. Yuan F, Qian L, Zhao X, Liu JY, Song L, et al. 2012. Fanconi anemia complementation group A (FANCA) protein has intrinsic affinity for nucleic acids with preference for single-stranded forms. *J. Biol. Chem.* 287:4800–7
110. Wang S, Wang R, Peralta C, Yaseen A, Pavletich NP. 2020. Structure of the Fanconi Anemia Core–UBE2T complex poised to ubiquitinate bound FANCI–FANCD2. bioRxiv 854158. **https://doi.org/10.1101/854158**
111. Huang Y, Leung JW, Lowery M, Matsushita N, Wang Y, et al. 2014. Modularized functions of the Fanconi anemia core complex. *Cell Rep.* 7:1849–57
112. Huang M, Kennedy R, Ali AM, Moreau LA, Meetei AR, et al. 2011. Human MutS and FANCM complexes function as redundant DNA damage sensors in the Fanconi anemia pathway. *DNA Repair* 10:1203–12
113. Williams SA, Wilson JB, Clark AP, Mitson-Salazar A, Tomashevski A, et al. 2011. Functional and physical interaction between the mismatch repair and FA-BRCA pathways. *Hum. Mol. Genet.* 20:4395–410
114. Ali AM, Pradhan A, Singh TR, Du C, Li J, et al. 2012. FAAP20: a novel ubiquitin-binding FA nuclear core-complex protein required for functional integrity of the FA-BRCA DNA repair pathway. *Blood* 119:3285–94
115. van Twest S, Murphy VJ, Hodson C, Tan W, Swuec P, et al. 2017. Mechanism of ubiquitination and deubiquitination in the Fanconi anemia pathway. *Mol. Cell* 65:247–59

116. Alpi AF, Pace PE, Babu MM, Patel KJ. 2008. Mechanistic insight into site-restricted monoubiquitination of FANCD2 by Ube2t, FANCL, and FANCI. *Mol. Cell* 32:767–77
117. Longerich S, San Filippo J, Liu D, Sung P. 2009. FANCI binds branched DNA and is monoubiquitinated by UBE2T-FANCL. *J. Biol. Chem.* 284:23182–86
118. Rajendra E, Oestergaard VH, Langevin F, Wang M, Dornan GL, et al. 2014. The genetic and biochemical basis of FANCD2 monoubiquitination. *Mol. Cell* 54:858–69
119. Shakeel S, Rajendra E, Alcon P, O'Reilly F, Chorev DS, et al. 2019. Structure of the Fanconi anaemia monoubiquitin ligase complex. *Nature* 575:234–37
120. Swuec P, Renault L, Borg A, Shah F, Murphy VJ, et al. 2017. The FA core complex contains a homodimeric catalytic module for the symmetric mono-ubiquitination of FANCI-FANCD2. *Cell Rep*. 18:611–23
121. Polito D, Cukras S, Wang X, Spence P, Moreau L, et al. 2014. The carboxyl terminus of FANCE recruits FANCD2 to the Fanconi anemia (FA) E3 ligase complex to promote the FA DNA repair pathway. *J. Biol. Chem*. 289:7003–10
122. Nookala RK, Hussain S, Pellegrini L. 2007. Insights into Fanconi anaemia from the structure of human FANCE. *Nucleic Acids Res*. 35:1638–48
123. Alcon P, Shakeel S, Chen ZA, Rappsilber J, Patel KJ, Passmore LA. 2020. FANCD2-FANCI is a clamp stabilized on DNA by monoubiquitination of FANCD2 during DNA repair. *Nat. Struct. Mol. Biol.* 27:240–48
124. Rennie ML, Lemonidis K, Arkinson C, Chaugule VK, Clarke M, et al. 2020. Differential functions of FANCI and FANCD2 ubiquitination stabilize ID2 complex on DNA. *EMBO Rep*. 21:e50133
125. Sato K, Toda K, Ishiai M, Takata M, Kurumizaka H. 2012. DNA robustly stimulates FANCD2 monoubiquitylation in the complex with FANCI. *Nucleic Acids Res*. 40:4553–61
126. Liang CC, Li Z, Lopez-Martinez D, Nicholson WV, Venien-Bryan C, Cohn MA. 2016. The FANCD2-FANCI complex is recruited to DNA interstrand crosslinks before monoubiquitination of FANCD2. *Nat. Commun.* 7:12124
127. Tan W, van Twest S, Leis A, Bythell-Douglas R, Murphy VJ, et al. 2020. Monoubiquitination by the human Fanconi anemia core complex clamps FANCI:FANCD2 on DNA in filamentous arrays. *eLife* 9:e54128
128. Cheung RS, Castella M, Abeyta A, Gafken PR, Tucker N, Taniguchi T. 2017. Ubiquitination-linked phosphorylation of the FANCI S/TQ cluster contributes to activation of the Fanconi anemia I/D2 complex. *Cell Rep*. 19:2432–40
129. Nijman SM, Huang TT, Dirac AM, Brummelkamp TR, Kerkhoven RM, et al. 2005. The deubiquitinating enzyme USP1 regulates the Fanconi anemia pathway. *Mol. Cell* 17:331–39
130. Cohn MA, Kowal P, Yang K, Haas W, Huang TT, et al. 2007. A UAF1-containing multisubunit protein complex regulates the Fanconi anemia pathway. *Mol. Cell* 28:786–97
131. Tan W, van Twest S, Murphy VJ, Deans AJ. 2020. ATR-mediated FANCI phosphorylation regulates both ubiquitination and deubiquitination of FANCD2. *Front. Cell Dev. Biol.* 8:2
132. Oestergaard VH, Langevin F, Kuiken HJ, Pace P, Niedzwiedz W, et al. 2007. Deubiquitination of FANCD2 is required for DNA crosslink repair. *Mol. Cell* 28:798–809
133. Kim JM, Parmar K, Huang M, Weinstock DM, Ruit CA, et al. 2009. Inactivation of murine Usp1 results in genomic instability and a Fanconi anemia phenotype. *Dev. Cell* 16:314–20
134. Matsushita N, Kitao H, Ishiai M, Nagashima N, Hirano S, et al. 2005. A FancD2-monoubiquitin fusion reveals hidden functions of Fanconi anemia core complex in DNA repair. *Mol. Cell* 19:841–47
135. Gibbs-Seymour I, Oka Y, Rajendra E, Weinert BT, Passmore LA, et al. 2015. Ubiquitin-SUMO circuitry controls activated fanconi anemia ID complex dosage in response to DNA damage. *Mol. Cell* 57:150–64
136. Husnjak K, Dikic I. 2012. Ubiquitin-binding proteins: decoders of ubiquitin-mediated cellular functions. *Annu. Rev. Biochem.* 81:291–322
137. Semlow DR, Zhang J, Budzowska M, Drohat AC, Walter JC. 2016. Replication-dependent unhooking of DNA interstrand cross-links by the NEIL3 glycosylase. *Cell* 167:498–511
138. Liu M, Bandaru V, Bond JP, Jaruga P, Zhao X, et al. 2010. The mouse ortholog of NEIL3 is a functional DNA glycosylase in vitro and in vivo. *PNAS* 107:4925–30

139. Dewar JM, Walter JC. 2017. Mechanisms of DNA replication termination. *Nat. Rev. Mol. Cell Biol.* 18:507–16
140. Atamna H, Cheung I, Ames BN. 2000. A method for detecting abasic sites in living cells: age-dependent changes in base excision repair. *PNAS* 97:686–91
141. Sejersted Y, Hildrestrand GA, Kunke D, Rolseth V, Krokeide SZ, et al. 2011. Endonuclease VIII-like 3 (Neil3) DNA glycosylase promotes neurogenesis induced by hypoxia-ischemia. *PNAS* 108:18802–7
142. Massaad MJ, Zhou J, Tsuchimoto D, Chou J, Jabara H, et al. 2016. Deficiency of base excision repair enzyme NEIL3 drives increased predisposition to autoimmunity. *J. Clin. Investig.* 126:4219–36
143. Hodskinson MR, Bolner A, Sato K, Kamimae-Lanning AN, Rooijers K, et al. 2020. Alcohol-derived DNA crosslinks are repaired by two distinct mechanisms. *Nature* 579:603–8
144. Dronkert ML, Kanaar R. 2001. Repair of DNA interstrand cross-links. *Mutat. Res.* 486:217–47
145. Bessho T, Mu D, Sancar A. 1997. Initiation of DNA interstrand cross-link repair in humans: the nucleotide excision repair system makes dual incisions 5′ to the cross-linked base and removes a 22- to 28-nucleotide-long damage-free strand. *Mol. Cell. Biol.* 17:6822–30
146. Ishiai M, Kimura M, Namikoshi K, Yamazoe M, Yamamoto K, et al. 2004. DNA cross-link repair protein SNM1A interacts with PIAS1 in nuclear focus formation. *Mol. Cell. Biol.* 24:10733–41
147. Kato N, Kawasoe Y, Williams H, Coates E, Roy U, et al. 2017. Sensing and processing of DNA interstrand crosslinks by the mismatch repair pathway. *Cell Rep.* 21:1375–85
148. Williams HL, Gottesman ME, Gautier J. 2012. Replication-independent repair of DNA interstrand crosslinks. *Mol. Cell* 47:140–47
149. Smeaton MB, Hlavin EM, McGregor Mason T, Noronha AM, Wilds CJ, Miller PS. 2008. Distortion-dependent unhooking of interstrand cross-links in mammalian cell extracts. *Biochemistry* 47:9920–30
150. Enoiu M, Jiricny J, Scharer OD. 2012. Repair of cisplatin-induced DNA interstrand crosslinks by a replication-independent pathway involving transcription-coupled repair and translesion synthesis. *Nucleic Acids Res.* 40:8953–64
151. Vermeulen W, Fousteri M. 2013. Mammalian transcription-coupled excision repair. *Cold Spring Harb. Perspect. Biol.* 5:a012625
152. Iyama T, Lee SY, Berquist BR, Gileadi O, Bohr VA, et al. 2015. CSB interacts with SNM1A and promotes DNA interstrand crosslink processing. *Nucleic Acids Res.* 43:247–58
153. Lopez-Martinez D, Liang CC, Cohn MA. 2016. Cellular response to DNA interstrand crosslinks: the Fanconi anemia pathway. *Cell Mol. Life Sci.* 73:3097–114
154. Cole RS. 1970. Light-induced cross-linking of DNA in the presence of a furocoumarin (psoralen). Studies with phage λ, *Escherichia coli*, and mouse leukemia cells. *Biochim. Biophys. Acta* 217:30–39
155. Spielmann HP, Dwyer TJ, Hearst JE, Wemmer DE. 1995. Solution structures of psoralen monoadducted and cross-linked DNA oligomers by NMR spectroscopy and restrained molecular dynamics. *Biochemistry* 34:12937–53
156. Gruppi F, Hejazi L, Christov PP, Krishnamachari S, Turesky RJ, Rizzo CJ. 2015. Characterization of nitrogen mustard formamidopyrimidine adduct formation of bis(2-chloroethyl)ethylamine with calf thymus DNA and a human mammary cancer cell line. *Chem. Res. Toxicol.* 28:1850–60
157. Rink SM, Solomon MS, Taylor MJ, Rajur SB, McLaughlin LW, Hopkins PB. 1993. Covalent structure of a nitrogen mustard-induced DNA interstrand cross-link: an N7-to-N7 linkage of deoxyguanosine residues at the duplex sequence 5′-d(GNC). *J. Am. Chem. Soc.* 115:2551–57
158. Osborne MR, Lawley PD. 1993. Alkylation of DNA by melphalan with special reference to adenine derivatives and adenine-guanine cross-linking. *Chem. Biol. Interact.* 89:49–60
159. Fischhaber PL, Gall AS, Duncan JA, Hopkins PB. 1999. Direct demonstration in synthetic oligonucleotides that *N*,*N*′-bis(2-chloroethyl)-nitrosourea cross links N^1 of deoxyguanosine to N^3 of deoxycytidine on opposite strands of duplex DNA. *Cancer Res.* 59:4363–68
160. Wang M, McIntee EJ, Cheng G, Shi Y, Villalta PW, Hecht SS. 2000. Identification of DNA adducts of acetaldehyde. *Chem. Res. Toxicol.* 13:1149–57
161. Cho YJ, Wang H, Kozekov ID, Kurtz AJ, Jacob J, et al. 2006. Stereospecific formation of interstrand carbinolamine DNA cross-links by crotonaldehyde- and acetaldehyde-derived α-CH_3-γ-OH-1,N^2-propano-2′-deoxyguanosine adducts in the 5′-CpG-3′ sequence. *Chem. Res. Toxicol.* 19:195–208

162. Price NE, Johnson KM, Wang J, Fekry MI, Wang Y, Gates KS. 2014. Interstrand DNA-DNA cross-link formation between adenine residues and abasic sites in duplex DNA. *J. Am. Chem. Soc.* 136:3483–90
163. Niedernhofer LJ, Daniels JS, Rouzer CA, Greene RE, Marnett LJ. 2003. Malondialdehyde, a product of lipid peroxidation, is mutagenic in human cells. *J. Biol. Chem.* 278:31426–33
164. Kirchner JJ, Sigurdsson ST, Hopkins PB. 1992. Interstrand cross-linking of duplex DNA by nitrous acid: covalent structure of the dG-to-dG cross-link at the sequence 5′-CG. *J. Am. Chem. Soc.* 114:4021–27
165. Wolkenberg SE, Boger DL. 2002. Mechanisms of in situ activation for DNA-targeting antitumor agents. *Chem. Rev.* 102:2477–95
166. Zhao Q, He Q, Ding W, Tang M, Kang Q, et al. 2008. Characterization of the azinomycin B biosynthetic gene cluster revealing a different iterative type I polyketide synthase for naphthoate biosynthesis. *Chem. Biol.* 15:693–705
167. Armstrong RW, Salvati ME, Nguyen M. 1992. Novel interstrand cross-links induced by the antitumor antibiotic carzinophillin/azinomycin. *B. J. Am. Chem. Soc.* 114:3144–45
168. Nougayrède JP, Homburg S, Taieb F, Boury M, Brzuszkiewicz E, et al. 2006. *Escherichia coli* induces DNA double-strand breaks in eukaryotic cells. *Science* 313:848–51

Annual Review of Biochemistry
Volume 90, 2021

Contents

Errata

An online log of corrections to *Annual Review of Biochemistry* articles may be found at http://www.annualreviews.org/errata/biochem